Title	Novel Power Allocation Grouping Scheme with NOMA for Multi-User Visible Light Communication
Author(s)	涂, 洋
Citation	
Issue Date	2025-03
Type	Thesis or Dissertation
Text version	author
URL	http://hdl.handle.net/10119/19807
Rights	
Description	Supervisor: リム 勇仁, 先端科学技術研究科, 修士 (情報科学)

Master's Thesis

Novel Power Allocation Grouping Scheme with NOMA for Multi-User Visible Light Communication

TU Yang

Supervisor Associate Professor Yuto LIM
Second Supervisor Professor Yasuo TAN

Graduate School of Advanced Science and Technology
Japan Advanced Institute of Science and Technology
Master of Science (Information Science)

March 2025

NOVEL POWER ALLOCATION GROUPING SCHEME WITH NOMA FOR MULTI-USER VISIBLE LIGHT COMMUNICATION

By TU Yang (2310111)

A thesis submitted to
School of Information Science,
Japan Advanced Institute of Science and Technology,
in partial fulfillment of the requirements
for the degree of
Master of Science

Supervisor :	Associate Professor LIM, Yuto
Main Examiner :	Associate Professor LIM, Yuto
Examiners :	Professor TAN, Yasuo
	Professor KURKOSKI, Brian Michael
	Senior Lecturer He, Cuiwei

Graduate School of Advanced Science and Technology
Japan Advanced Institute of Science and Technology
(Information Science)

March 2025

Abstract

Visible Light Communication (VLC) using white Light Emitting Diode (LED)s for both indoor illumination and wireless data transmission is expected to play an important role in future generations of wireless communication networks due to its many advantages, such as the low cost of transceivers, the unregulated optical spectrum, and the secure nature of the transmission. Despite these advantages, one challenge is that when commercially available white LEDs are used as data transmitters, their modulation bandwidth is typically limited to only a few MHz. This limitation could constrain the transmission data rate, particularly when a single LED luminaire needs to support multiple users.

One potential solution to overcome this bottleneck problem is to use non-orthogonal multiple access Non Orthogonal Multiple Access (NOMA). In radio frequency (RF) wireless communication systems, NOMA has been shown to be a highly efficient approach for improving the spectral efficiency of wireless transmission systems, at the cost of increased demodulation complexity on the receiver side, as data demodulation follows a Successive Interference Cancellation (SIC) process. Despite NOMA's success in RF wireless systems, its study in VLC or optical wireless communication remains limited. This is because VLC typically uses Intensity Modulation (IM)/Direct Detection (DD), and the transmitted signal must be constrained to be both real and unipolar. Therefore, many NOMA techniques used in RF cannot be directly applied to VLC without significant modifications.

This thesis focuses on the implementation of NOMA in VLC and its integration with Orthogonal Frequency Division Multiple (OFDM) modulation, which is the modulation scheme used in most VLC standards. Specifically, the contributions of this thesis are divided into two stages. In the first stage, NOMA is integrated with an optical OFDM modulation scheme called Asymmetrically Clipped DC biased Optical (ADO) OFDM (ADO-OFDM), considering a special case where two users are paired. This approach differs from the conventional ADO-OFDM scheme, which is designed to support only a single user. In the proposed ADO-OFDM NOMA scheme, the odd subcarriers, modulated with the Asymmetrically Clipped Optical (ACO) OFDM (ACO-OFDM) component, carry the data intended for the user located farthest from the LED transmitter. Meanwhile, the data for the user closer to the LED transmitter is modulated onto the even subcarriers, which are modulated with the Direct Current biased Optical (DCO) OFDM (DCO-OFDM) component. Furthermore, unlike conventional ADO-OFDM, the concept of NOMA is incorporated. The signal components of ACO-OFDM and DCO-OFDM are assigned different power levels based on the users' locations to balance performance between them. Simulation results show that by optimizing the power ratios between these two signal components, the overall Bit Error Rate (BER) can be significantly reduced.

In the second stage of this study, the proposed ADO-OFDM NOMA scheme is extended to a general case where a large number of users need to be supported. Specifically, the users are divided into multiple groups, with each group containing four users. To group the users efficiently, a grouping algorithm called Minimizing Channel Gain Average Difference (MCGAD) is proposed. This algorithm depends on the channel gain of individual users, where the two users with higher channel gains are grouped with the two users with lower channel gains. Within each group, the four users are further divided into two pairs, with each pair implementing ADO-OFDM NOMA individually. Furthermore, an algorithm is developed to determine the optimal power allocation ratio between each user pair, as well as the power ratio of individual users within each pair. Simulation results show that by using the new grouping method together with the algorithm to allocate the optimal power ratio, the spectral efficiency of the system can be significantly improved.

In summary, this thesis makes a significant contribution by implementing NOMA techniques in VLC to enable multi-user support through a single LED transmitter. It also explores the integration of NOMA with optical OFDM modulation. Additionally, novel Digital Signal Processing (DSP) techniques and advanced power allocation algorithms are proposed and analyzed to optimize transmission performance. Simulation results are provided to validate the effectiveness of the proposed methods, demonstrating their potential in improving the performance of VLC systems.
Keywords: VLC, NOMA, ACO-OFDM, DCO-OFDM, ADO-OFDM, MCGAD, Subcarrier Partitioning, SIC, Spectral Efficiency, Energy Efficiency

Acknowledgement

Above all, my deepest appreciation goes to my primary supervisor Associate Professor Yuto LIM. His patient guidance and unwavering support have been invaluable throughout this research journey. His genuine warmth and dedication have profoundly inspired me, and his generosity has made my experience at JAIST truly enriching. I am also sincerely grateful to my second supervisor Professor Yasuo TAN, whose steady encouragement has fueled my resolve and sustained my commitment to completing this study.

In addition, I would like to extend my deepest gratitude to Senior Lecturer Cuiwei HE for his invaluable technical guidance and generous assistance. His professional expertise and willingness to share knowledge have greatly enhanced the rigor of my research, deepened my understanding of the subject matter, and provided me with significant academic support.

Special thanks are due to Professor NGUYEN, Minh Le for his patient mentorship and guidance during my minor research in Artificial Intelligence. His insightful teachings not only helped me acquire essential expertise but also fostered significant personal growth in this emerging field. I am likewise deeply grateful to Professor Kurkosiki, Brian Michael, who generously found time in a demanding schedule to thoroughly review my thesis and offer incisive feedback during my defense. His thoughtful suggestions allowed me to view my work from new angles and gain a deeper understanding of its research implications.

I am further appreciative of the researchers from TAN Laboratory and LIM Laboratory at JAIST for their invaluable assistance and keen insights during our collaborative discussions. Their genuine camaraderie and willingness to share expertise made my tenure as a student both productive and enjoyable. I also owe gratitude to Dr. Cui Zhihan, a senior colleague in my lab, for his generous sharing of knowledge and consistent guidance throughout my master's program, as well as during the writing of this thesis.

Lastly, heartfelt thanks go to everyone who offered direct or indirect support in helping me reach this academic milestone. Above all, I remain profoundly thankful to my family for their steadfast love and encouragement, which have empowered me to chart a brighter path forward on my own.

Contents

List of Figures

List of Tables

List of Symbols

The following list describes several symbols that are used within the body of this document:

α Power allocation factor of the NOMA power allocation Ratio

β Power allocation factor of the ADO power allocation Ratio

ϕ Angle of emission relative to the LED's optical axis

$\phi_{1/2}$ Half-intensity angle (i.e., the angle at which the LED's radiant intensity is half of its peak value)

ϕ_k Emission angle from the LED transmitter to the kth user

ψ Angle of incidence at the receiver (e.g., photodiode)

Ψ_{c} Represents the PD's field-of-view (FOV)

ψ_{FOV} Field-of-view angle of the photodiode (PD)

A Effective receiving area of the photodiode (PD)

B Channel bandwidth

d_k Direct distance between the kth user and the LED

H Overall channel gain

$H^{(ado)}$ Each user *ado* may experience a distinct channel gain

h^k channel gain of the kth reflection path

m Lambertian order determined by $\phi_{1/2}$, characterizing the LED's emission profile

n	Additive White Gaussian Noise
n_k	Channel noise between the kth user and the LED transmitter
P_{r}	The received optical power at the photodiode (PD)
$P_{\mathrm{r}}^{(ado)}$	User ado's received power
P_{t}	Denotes the LED transmitted optical power
P_k	Power of the kth user
R_p	Responsivity of the photodiode (PD)
s_k	Transmitted signal of the kth user
SNR	Transmit signal-to-noise ratio

List of Abbreviations

ACO Asymmetrically Clipped Optical

ADO Asymmetrically Clipped DC biased Optical

AI Artificial Intelligence

BER Bit Error Rate

DCO Direct Current biased Optical

DD Direct Detection

DMT Discrete Multi-Tone

DSP Digital Signal Processing

FDM Frequency Division Multiplexing

GaN gallium nitride

IFFT Inverse Fast Fourier Transform

IM Intensity Modulation

IoT Internet of Things

ISI Inter-Symbol Interference

LED Light Emitting Diode

LiFi Light Fidelity

LOS Line of Sight

MCGAD Minimizing Channel Gain Average Difference

MIMO Multiple-Input and Multiple-Output

NLOS Non-Line-of-Sight

NOMA Non Orthogonal Multiple Access

OFDM Orthogonal Frequency Division Multiple

OMA Orthogonal Multiple Access

PAPR Peak-to-Average Power Ratio

PD Photodiodes

QAM Quadrature Amplitude Modulation

RF Radio Frequency

SIC Successive Interference Cancellation

SNR Signal-to-Noise Ratio

VLC Visible Light Communication

WDM Wavelength Division Multiplexing

WiFi Wireless Fidelity

Chapter 1

Introduction

With the rapid development of the Internet of Things (IoT) and Artificial Intelligence (AI) technologies, humanity is entering an era of intelligence marked by the "Internet of Everything." The explosion of big data has significantly heightened the demand for communication bandwidth, placing immense stress on existing commercial networks. Overcoming these challenges requires both upgrading current systems and investigating new communication resources.

Against this backdrop, a novel technology known as VLC has emerged, using abundant spectral resources in the visible-light range to address the scarcity inherent to traditional Radio Frequency (RF) communication [8]. In VLC systems, white LEDs installed in an indoor setting serve as transmitters; these LEDs are modulated via LED drivers to embed data into high speed intensity fluctuations imperceptible to the human eye. Photodiodes combined with current to voltage amplifiers capture the modulated light, and digital baseband units recover the data through modulation and demodulation processes. Compared to typical RF based systems, VLC offers high data rates, energy efficiency, and increased capacity, making it a promising green wireless communication solution.

Time magazine underscored the importance of VLC by listing it among the "50 Best Inventions" in 2011 [8]. Exploiting an optical spectrum of roughly 380 nm to 780 nm (see Figure 1.1) endows VLC with a broader bandwidth than RF systems, enabling data rates up to 10 Gb/s. Besides its wide bandwidth and high speed, VLC is comparatively cost effective. White LEDs are inexpensive, energy efficient, and long lasting; minimal alterations can

Table 1.1: Comparison of Radio and VLC Systems

Property	**Radio System**	**VLC System**
Bandwidth Regulated	Yes	No
Security	Low	High
RF Electromagnetic Interference	Yes	No
Passes Through Walls	Yes	No
Technology Cost	High	Low
Beam Directionality	Low	Medium
Available Bandwidth	Low	Very High
Transmitted Power	Interference	Eye safety, Interference
Noise Sources	Other Users and Systems	Sunlight, Ambient Light
Power Consumption	Medium	Relatively Low
Multipath Fading	Yes	No

realize dual functionalities for illumination and communication. As a result, VLC is viewed as an attractive option for future high-speed and high capacity requirements, including intelligent lighting, indoor positioning, and large scale IoT applications.

One prominent benefit of VLC lies in its high level of security: visible light does not penetrate solid walls, effectively confining coverage within a given space and reducing eavesdropping risks. Additionally, VLC operates without spectrum licensing constraints, circumventing the regulatory burdens commonly faced by RF communication. Furthermore, VLC is immune to electromagnetic interference, making it suitable for sensitive environments such as hospitals, airplanes, and gas stations. Despite these advantages, limitations exist. The restricted modulation bandwidth of typical LEDs can limit system capacity, and the inability of visible light to pass through obstacles can lead to disrupted signals. Accordingly, VLC is seen as both a strong supplement and a viable alternative to conventional indoor wireless communication systems.

To further advance VLC, researchers have explored NOMA, which enhances spectrum utilization and supports multi-user connectivity [9, 10].

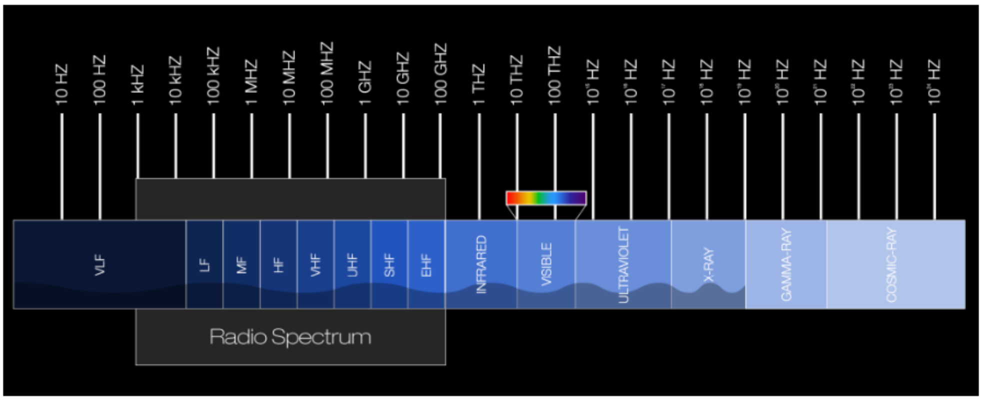

Figure 1.1: Visible light spectrum [1].

Among various NOMA approaches, power domain NOMA (PD-NOMA) excels for its spectrum efficiency [11]. Integrating PD-NOMA with VLC offers a promising route to boost multi-user performance, providing a novel solution for indoor wireless communication.

This chapter primarily concentrates on optimizing power allocation in multi-user NOMA VLC systems, as power distribution and spectrum efficiency critically affect both system performance and user fairness. The central goal is to propose strategies that alleviate existing challenges and advance indoor wireless communication.

1.1 Historical Developments in VLC

As society and technology progress, VLC has garnered considerable attention as an emerging wireless communication method. Research worldwide has led to numerous breakthroughs. Proposed initially in 2000 by M. Nakagawa and colleagues at Keio University, VLC was systematically analyzed in 2002 concerning light-source models, channel characteristics, and Signal-to-Noise Ratio (SNR) [12]. By 2004, M. Nakagawa and Komine *et al.* delved into Inter-Symbol Interference (ISI) resulting from path-length discrepancies in multi-light-source scenarios [13].

To accelerate standardization and facilitate practical deployment, Japan established the Visible Light Communications Consortium (VLCC) in 2003, comprising notable firms in communication and lighting. In 2007, VLCC released standards for VLC systems and visible-light identification, spurring widespread industry adoption [14]. Concurrently, the European Union (EU) initiated the OMEGA project in 2008 to attain Gbit/s data rates in home-access networks [15]. In 2009, the Fraunhofer Institute in Germany, in collaboration with Siemens, presented a VLC link running at 200 Mbit/s and exhibiting low bit error rates [16]. That same year, Hoa Le Minh *et al.* at the University of Oxford attained 100 Mbit/s via post-equalization [17]. By 2010, multiple Multiple-Input and Multiple-Output (MIMO) schemes with Orthogonal Frequency Division Multiple (OFDM) pushed throughput to 220 Mbit/s [18], while around the same time Vucic J *et al.* in Germany achieved 531 Mbit/s using Discrete Multi-Tone (DMT) [19]. In 2011, incorporating Wavelength Division Multiplexing (WDM) on an RGB LED raised data rates to 803 Mbit/s [20], and Prof. Harald Haas of the University of Edinburgh introduced the term "Li-Fi" as he discussed its potential applications, later founding Pure LiFi to commercialize VLC [21].

Further developments saw Khalid A. M *et al.* employing adaptive-rate DMT in 2012 to achieve 1 Gbit/s on a single fluorescent white LED [22]. In 2014, Tsonev D *et al.* harnessed gallium nitride (GaN) LEDs with equalization, adaptive bit-loading, and Orthogonal Frequency Division Multiple, reaching 3 Gbit/s a record at that time for single-color LEDs [23]. By 2016, Chun H *et al.* used WDM and OFDM on an RGB LED to validate 10 Gbit/s over 1.5 m [24]. In 2018, Beysens J *et al.* proposed DenseVLC, a large scale Multiple-Input and Multiple-Output (MIMO) framework featuring densely distributed LEDs in a cell free arrangement [25]. That same year, Wang J *et al.* introduced a more accurate path-loss channel model for VLC using recursive formulations [26]. In 2020, Wu X *et al.* developed a load-balancing method tailored to heterogeneous Light Fidelity (LiFi)/Wireless Fidelity (WiFi) networks, increasing system throughput by 68% under high mobility or frequent blockages [27].

From Japan's initial vision to extensive research efforts in Europe, Germany, the UK, and beyond, VLC has progressed rapidly. Demonstrations surpassing Gbit/s speeds, along with evolving industrial standards, underscore its considerable potential to mitigate bandwidth and spectrum shortages in wireless communications. As shown in Figure 1.2, VLC is poised for an increasingly prominent role in next-generation indoor networks and diverse Internet of Things-centric applications.

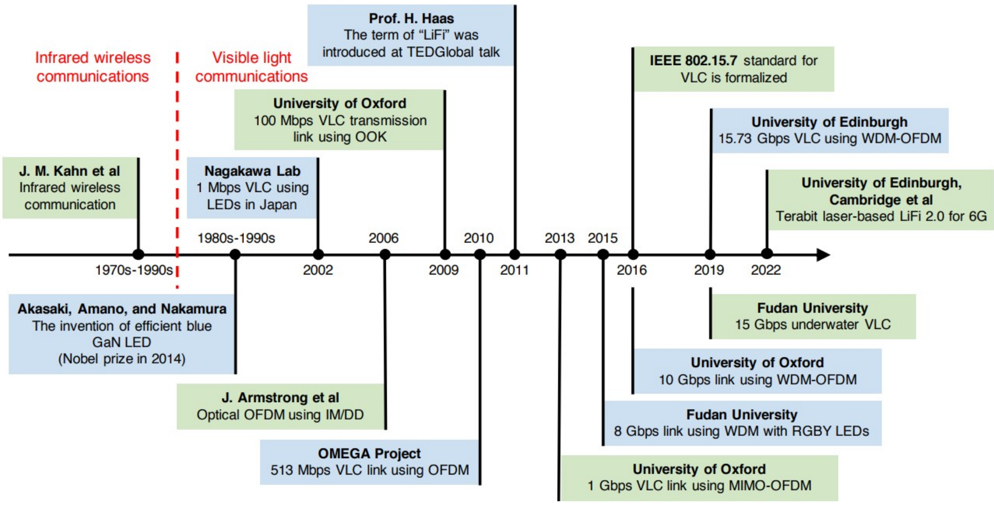

Figure 1.2: VLC research milestones [2].

An LED-based VLC system can serve both illumination and data transmission functions in future wireless networks (see Figure 1.3) [28]. Because the LED emission is incoherent, intensity modulation/direct detection (IM/DD) is typically employed [29]. Under IM/DD, the voltage or current driving the LED must be real and non-negative, which necessitates specialized optical OFDM techniques [4, 30, 31]. In both DCO-OFDM and ACO-OFDM, Quadrature Amplitude Modulation (QAM) symbols must follow Hermitian symmetry to generate real time domain signals, but these methods differ in how they achieve unipolar output.

- **DCO-OFDM**: Adds a DC bias to make all signal amplitudes positive, but high Peak-to-Average Power Ratio (PAPR) often demands an excessive bias, reducing power efficiency [32].

- **ACO-OFDM**: Transmits data exclusively on odd subcarriers, allowing negative samples to be clipped at zero without distortion. Although more power-efficient, ACO-OFDM utilizes only half the spectrum, limiting spectral efficiency [33].

To balance power and spectral efficiency, a hybrid scheme known as ADO-OFDM was proposed [34], wherein ACO-OFDM signals occupy the odd subcarriers and DCO-OFDM signals occupy the even subcarriers.

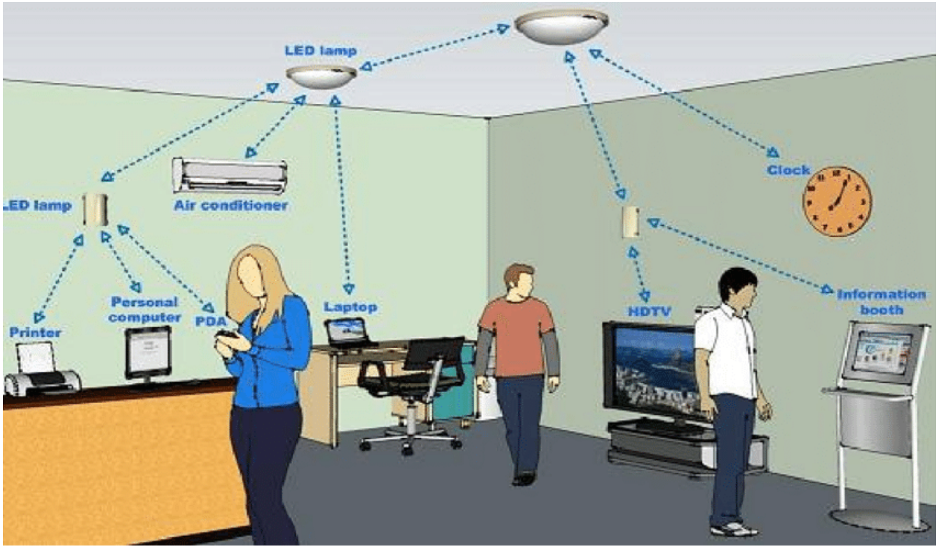

Figure 1.3: Indoor VLC system with LED illumination and data transmission [3].

This chapter highlights core challenges in VLC systems and outlines key strategies for improving their performance in forthcoming communication networks. The primary objective is to design a multi-user transmission framework that merges spectrally efficient modulation methods with NOMA. By addressing current limitations in LED bandwidth and system interruptions caused by LOS blockage, the study seeks to improve spectral efficiency across multiple users.

Specifically, the research investigates the power distribution mechanism in a joint spectrally efficient modulation and NOMA setting, ensuring fair resource allocation among users with significantly different channel conditions. Additionally, the proposed approach aims to support an increased number of user devices while preserving high data rates. Overcoming these technical barriers will enhance VLC's suitability for future indoor wireless applications.

In the following section, the major milestones in the VLC development are summarized and discussed in detail.

1.2 Problem Statement

As demand for high speed and efficient wireless data transmission grows, VLC has drawn attention due to its abundant spectrum resources, high security, and immunity to electromagnetic interference. However, accommodating an increasing number of users in VLC systems introduces significant challenges that must be addressed to fully exploit its potential in multi-user scenarios.

The first challenge arises from limited shared resources, leading to inter-user interference and inefficient utilization. Although VLC's LOS coverage and inability to penetrate walls enable spatial spectrum reuse, in dense user environments overlapping transmissions degrade performance. Consequently, effective power allocation becomes critical, as users often experience significantly different channel conditions based on their proximity to the LED source.

A second issue relates to increased latency and reduced fairness in multi-user data transmission. When users with varying channel conditions compete for shared resources, maintaining low latency while ensuring fairness becomes a complex problem, necessitating careful resource allocation and user prioritization strategies.

To address these challenges, this research integrates NOMA with spectrally efficient ADO-OFDM modulation in VLC systems. The main objective is to develop a multi-user transmission framework that enhances spectral efficiency, ensures fair resource allocation, and minimizes latency. NOMA allows multiple users to share the same frequency band via different power levels, while ADO-OFDM achieves high data rates and spectral efficiency. This study further explores power-allocation mechanisms to optimize system throughput and uphold fairness for users with diverse channel conditions, thereby advancing VLC as a robust solution for multi-user communication environments.

1.3 Related Works and Motivation

VLC has attracted substantial research interest as an alternative to RF systems, because of its large available spectrum, high speed potential, and immunity to electromagnetic interference. Early studies mainly investigated high speed transmission through advanced modulation techniques, notably OFDM and its variants (e.g., ACO-OFDM and DCO-OFDM). These methods established a foundation for spectrally efficient VLC by enhancing data throughput while mitigating clipping noise.

As VLC evolved to support multiple users, NOMA emerged as an effective approach to improve spectral efficiency and user connectivity. By assigning different power levels according to channel conditions, NOMA enables multiple users to share the same frequency band more efficiently than conventional Orthogonal Multiple Access (OMA). However, most NOMA based VLC studies have been limited to two-user scenarios, leaving substantial scope for exploring more complex multi-user environments.

A key issue in multi-user VLC systems is user pairing, which defines how users share resources. Various grouping and power allocation strategies have been proposed. For instance, the multi-user grouping schemes in [5] aim to maximize channel gain differences for enhanced successive interference cancellation, but can become suboptimal when channel conditions vary widely. Similarly, iterative power allocation algorithms in [6] have shown potential to improve system throughput and energy efficiency, yet they may converge slowly or reach local optima in large-scale deployments. Another approach in [7] employs k-means clustering for resource allocation in multi-lamp, multi-user VLC systems, though it can incur high computational overhead and rely on careful parameter tuning.

Despite these developments, few studies have explored combining NOMA with ADO-OFDM in multi-user VLC. ADO-OFDM offers advantages in minimizing clipping noise and improving spectral efficiency, which can synergize with the multi-user multiplexing gains of NOMA. Most existing work instead focuses on either standalone OFDM schemes or simpler NOMA setups, creating a gap in the literature for dense VLC networks where user distributions and channel conditions can be highly dynamic.

Another limitation of conventional pairing and power allocation methods is their lack of attention to VLC specific factors, such as user positioning and orientation relative to LED sources. Overlooking these factors can lead to inefficient resource usage, unfair data-rate distribution, and decreased throughput problems that intensify under heavy interference or in large scale networks with overlapping signals. These conditions underscore the need for more adaptable and efficient solutions.

In light of these findings, this research aims to unify NOMA and ADO-OFDM in multi-user VLC systems, thus exploiting the potential advantages of both technologies. NOMA's ability to accommodate multiple users, combined with ADO-OFDM robustness against clipping noise, promises enhanced spectral and energy efficiency. In particular, incorporating a user-pairing mechanism such as Minimizing Channel Gain Average Difference (MCGAD) is expected to reduce complexity, adapt to varying channels, and ensure equitable resource allocation. By bridging existing gaps in the literature, this work endeavors to optimize scalability and overall performance in dense multi-user VLC scenarios, moving VLC closer to a high capacity, energy efficient, and user friendly communication technology.

1.4 Research Objectives

The objectives of this thesis are:

- To design a novel asymmetrically clipped DC biased optical (ADO) approach for NOMA based VLC system [34];
- To significantly enhance the spectral efficiency and energy efficiency in multiuser NOMA ADO approach based on grouping scheme, called MCGAD.

1.5 Research Approach

This work proposes a multi-user VLC framework that unifies NOMA with an ADO-OFDM approach by merging ACO-OFDM and DCO-OFDM into a single scheme. Users with relatively stronger channels are assigned ACO-OFDM to exploit lower power requirements and minimal clipping noise, whereas those with weaker channels use DCO-OFDM to accommodate higher data rates. Under this integrated design, NOMA based power allocation dynamically distributes transmit power according to each user's channel quality: stronger channel users receive less power to reduce interference, and weaker channel users receive more power to maintain fairness and throughput. At the receiver, SIC enables strong channel users to first decode and subtract the signals of weaker channel users who typically have higher power allocations before retrieving their data, while weaker channel users can directly decode their signals.

To further refine resource allocation, an MCGAD grouping mechanism organizes users by channel conditions, ensuring that users with similar channel strengths form groups where ACO-OFDM and DCO-OFDM assignments are managed more efficiently. In this process, distinct power ratio parameters α and β are derived to optimize both energy efficiency and spectral performance, adapting dynamically as users move or channel states change. The proposed framework is evaluated through realistic indoor VLC simulations, measuring spectral efficiency, bit error rate, throughput, and fairness. Results confirm that combining NOMA with ACO-OFDM and DCO-OFDM enhanced by an MCGAD grouping strategy provides a robust, high capacity solution for dense multi-user VLC networks. By capitalizing on ACO-OFDM energy efficiency and DCO-OFDM high data rate capability, the system addresses key challenges in multi-user indoor communication and paves the way for scalable VLC deployments.

1.6 Research Methodology

The research methodology is designed to evaluate and improve the performance of the multi-user NOMA VLC system, as illustrated in the workflow shown in the following Figure 1.4.

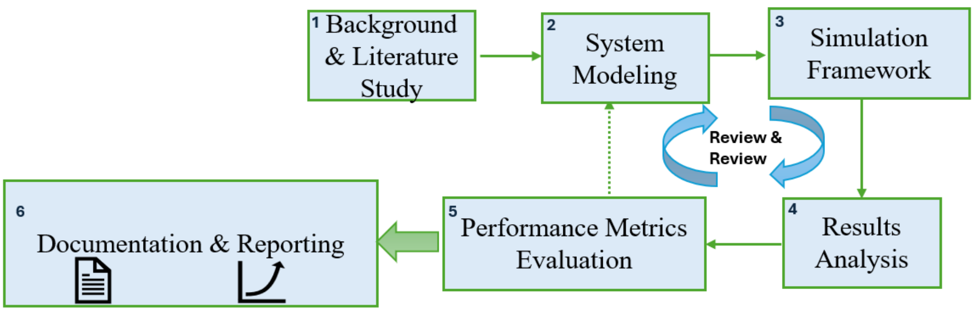

Figure 1.4: 6-step research methodology

The proposed methodology consists of a six-step process designed to thoroughly evaluate and improve the multi-user VLC system using the combination of ACO-OFDM, DCO-OFDM, and NOMA. The methodology is iterative, ensuring that system models are continuously refined and optimized.

The process begins with the Background and Literature Study, where existing studies on VLC systems, modulation techniques, and NOMA are reviewed. This step establishes a solid foundation for identifying challenges and gaps in the current state of the art, helping to define the research objectives and approaches.

In the System Modeling stage, we develop the theoretical framework of the VLC system and use the Lambertian transmission model to characterize the radiation pattern of LED transmitters, and user channel conditions are modeled based on their varying positions in an indoor environment. Additionally, interference models and power allocation strategies are designed to account for multi-user scenarios, incorporating ACO-OFDM for odd numbered users and DCO-OFDM for even numbered users.

Following the system modeling, a simulation framework is implemented using tools like MATLAB and Python. In this phase, theoretical models are validated through numerical simulations, which evaluate system performance in terms of capacity, BER, and user fairness. Various scenarios are simulated, including optimized power allocation schemes and user grouping strategies, to assess the effectiveness of the proposed methods.

The results of the simulation are then analyzed in the results analysis phase. Performance metrics such as BER, achievable data rates, and power allocation efficiency are visualized through graphs and compared with related work. This analysis helps identify areas for improvement, leading to iterative refinement of the system models.

The Performance metrics evaluation stage involves evaluating the system against established benchmarks and evaluating the impact of key parameters, such as power allocation coefficients and modulation schemes, on overall performance. The iterative nature of the methodology ensures continuous improvement through repeated cycles of simulation and analysis.

Finally, the results are documented in the documentation and reporting phase. A comprehensive research report and thesis are prepared, summarizing the findings, methodologies, and contributions of the study. This structured and iterative approach ensures that the proposed multi-user VLC system is rigorously evaluated and optimized for practical applications.

1.7 Thesis Organization

The thesis is organized into five chapters, each systematically addressing the proposed research on multi-user NOMA-based VLC systems. The objectives include designing a novel ADO-OFDM approach for NOMA based VLC systems and significantly enhancing spectral and energy efficiency through a grouping scheme called MCGAD. The first objective focuses on a two-user system (User 1: ACO, User 2: DCO), while the second objective extends the system to four users (Users 1 and 3: ACO, Users 2 and 4: DCO). The details of the thesis are organized as follows:

Chapter 1 begins by explaining what VLC is and outlining its main advantages, such as abundant spectral resources, energy efficiency, and strong security. The chapter also traces the development of VLC technology, highlighting important milestones and the progress made so far. Although VLC offers many benefits, it still faces challenges in areas like interference management, resource allocation, and user grouping, especially when supporting multiple users at once. To address these issues, the chapter introduces an innovative approach that combines existing knowledge with new ideas, aiming to enhance system performance under dense user conditions. Finally, it concludes by summarizing the research goals and proposed methods, setting a clear direction for the remaining chapters.

Chapter 2 opens with an exploration of the characteristics of the VLC channel, discussing how light propagation, reflections, and obstacles influence signal strength and overall system performance. It then introduces the principles of OFDM in VLC, including ACO-OFDM and DCO-OFDM. These techniques play a crucial role in achieving high data rates and efficient bandwidth usage. The chapter also clarifies the concept of NOMA and its potential for improving spectral efficiency and accommodating multiple users in VLC networks. By reviewing existing power-allocation methods, user-grouping strategies, and various channel models, Chapter 2 presents fundamental concepts of multi-user VLC systems, covering the VLC channel, OFDM techniques, and the basics of NOMA, thus laying the groundwork for the proposed ADO-OFDM NOMA solution introduced in subsequent chapters.

Chapter 3 provides a detailed explanation of the theoretical framework and the proposed for the ADO-OFDM NOMA VLC system. First, it introduces the system model, where User 1 employs ACO-OFDM and User 2 employs DCO-OFDM, followed by the power allocation method and SIC to enhance performance. The model is then expanded to four-user and multi-user scenarios, where Users 1 and 3 adopt ACO-OFDM, and Users 2 and 4 adopt DCO-OFDM. A new grouping scheme, MCGAD is presented to improve resource allocation efficiency and fairness. This chapter concludes with a detailed discussion of the algorithms and flowcharts that implement the proposed solutions, targeting both spectral and energy efficiency objectives.

Chapter 4 presents simulation results and provides a thorough analysis using both numerical metrics and mathematical expressions. Specific simulation parameters, settings, and test scenarios are introduced to assess the proposed system under varied conditions. Performance is evaluated in terms of spectral efficiency, energy efficiency, BER, user fairness, and throughput. Both the two-user and four-user models are examined, and the influence of the MCGAD grouping scheme is compared against existing methods. Through these simulations and the relevant mathematical expressions, the chapter illustrates the proposed method's advantages and underscores its potential for real world experimental validation in VLC systems.

Chapter 5 concludes the thesis by summarizing the research contributions and findings, particularly the advantages of the ADO-OFDM based NOMA VLC system and the MCGAD grouping scheme in boosting multi-user communication efficiency. The chapter also underlines the broader impact of VLC technology and points out several future directions. These include scaling the system to support more users, employing multiple LED sources for enhanced coverage, and refining power allocation through AI driven algorithms. In addition, potential real-world experiments are suggested to validate the proposed methods in practical environments. By emphasizing both theoretical progress and practical feasibility, this chapter illustrates how the proposed approach can be extended and adapted for next-generation VLC systems.

This structure offers a clear progression from identifying research problems to presenting and validating solutions resulting in a well organized discussion that advances multi-user NOMA based VLC systems.

Chapter 2

Background

This chapter delves into the fundamental principles of VLC and NOMA, emphasizing how these two technologies can be combined to enhance spectral efficiency and accommodate multiple users. It begins by examining the VLC channel and the role of LED based illumination and data transmission in indoor environments. The discussion then shifts to OFDM variations tailored for VLC, highlighting why ACO-OFDM and DCO-OFDM are particularly suited to intensity modulation and direct detection. Finally, the chapter introduces the power domain concept of NOMA, explaining how SIC enables the effective separation of user signals. By laying out these technical foundations, Chapter 2 sets the stage for the integrated ADO-OFDM based NOMA approach explored in subsequent chapters.

2.1 Optical Channel in VLC

VLC uses LEDs to transmit data at visible wavelengths(roughly 400–700 nm), taking advantage of indoor lighting to support both illumination and communication. Since the channel mainly depends on Line of Sight (LOS) paths, any physical obstruction can significantly weaken or block signals. Moreover, ambient light sources such as other lamps or sunlight introduce background noise and can alter the Signal-to-Noise Ratio (SNR). In addition to these challenges, multipath reflections on walls and surfaces can cause fluctuations in received signal quality. As a result, achieving high data rates in VLC requires advanced modulation and robust detection methods that handle dynamic indoor or outdoor conditions. Addressing these factors is crucial for building scalable and reliable VLC systems that meet modern wireless communication demands.

2.1.1 Fundamentals of Light Propagation

This section outlines the system model and key assumptions for our indoor VLC setup. As shown in Fig. 2.1, we consider a single LED transmitter mounted on the ceiling, covering multiple photodiodes (PDs) located at user devices within its illumination area. The LED simultaneously provides lighting and data transmission, utilizing visible wavelengths (around 400–700 nm).

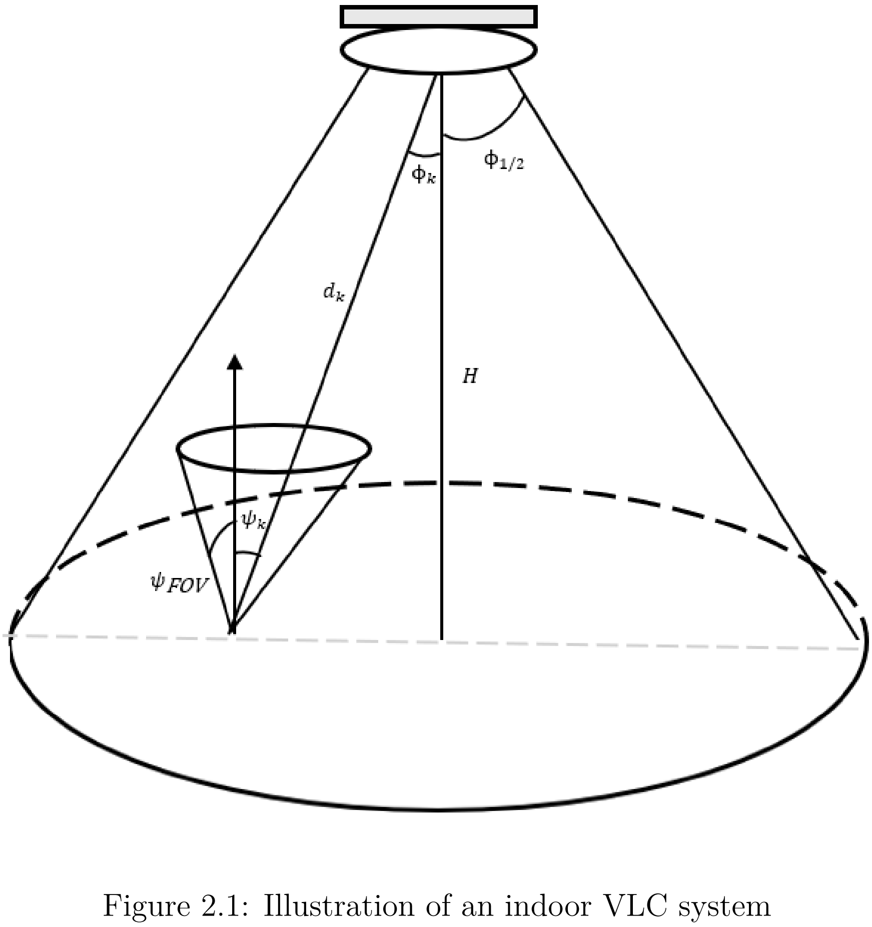

Figure 2.1: Illustration of an indoor VLC system

To describe how light propagates, we adopt a Lambertian assumption for the LED source, which means the emitted intensity follows a cosine pattern based on the emission angle. This model helps capture the angle dependent nature of LED output and the distribution of light across the room. When a PD receives the signal, its LOS path provides the strongest contribution, although reflections from walls or other surfaces may also play a role (see Fig. 2.2).

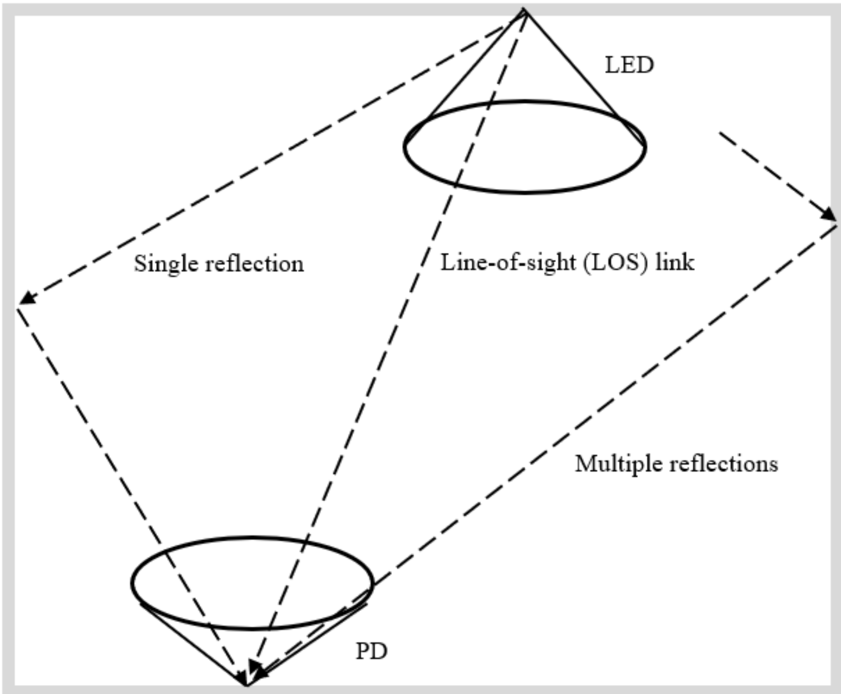

Figure 2.2: Main (LOS) and reflected (NLOS) paths in an indoor VLC setup

The complete optical channel gain can be written as

$$H = h^0 + h^1 + \cdots + h^k = \sum_{i=0}^{k} h^i$$

where h^0 represents the LOS component, and $h^1, \ldots, h^k$ account for reflections or other Non-Line-of-Sight (NLOS) paths. In practice, the LOS term often dominates, especially if the PD is significantly lower than the LED and remains unobstructed.

In real indoor environments, multiple reflections and other light sources can introduce interference. Users may also be positioned at different heights or angles, altering their channel conditions. Designing a robust VLC system thus requires careful handling of both direct and indirect paths, along with potential crosstalk from neighboring transmitters in more complex setups.

To evaluate performance, we typically express the achievable capacity based on the received signal power, noise level, and any interference present. The choice of modulation and multiple-access strategy (e.g., NOMA) further influences how throughput scales with the number of users. Sections to follow will detail these aspects, including the application of NOMA based techniques and relevant power allocation methods.

By focusing on these fundamental points LED emission characteristics, Lambertian channel modeling, and interference from reflections, we establish the core principles behind indoor VLC. These basics guide subsequent sections, where we introduce more advanced topics such as multi-user interference cancellation and resource allocation strategies.

2.1.2 Channel Model (Lambertian Source)

Under typical indoor conditions, the LOS path from an LED to a Photodiodes (PD) provides the strongest signal [35]. In this work, we assume a generalized Lambertian radiation model [36], where the radiant intensity $I(\phi)$ follows Lambert's cosine law with emission angle ϕ. Specifically,

$$I(\phi) \;=\; \frac{m+1}{2\pi}\, P_t \,\cos^m(\phi), \quad 0 \leq \phi \leq \tfrac{\pi}{2}, \tag{2.1}$$

where P_t is the transmitted optical power, and m is the Lambertian order determined by the LED's half power angle $\phi_{1/2}$:

$$m = -\frac{\ln(2)}{\ln\!\Big(\cos(\phi_{1/2})\Big)} \tag{2.2}$$

A larger m indicates a narrower beamwidth and stronger directionality. As shown in Fig. 2.3, different $\phi_{1/2}$ values yield different Lambertian patterns.

When the PD is at distance d from the LED under a clear LOS path, the

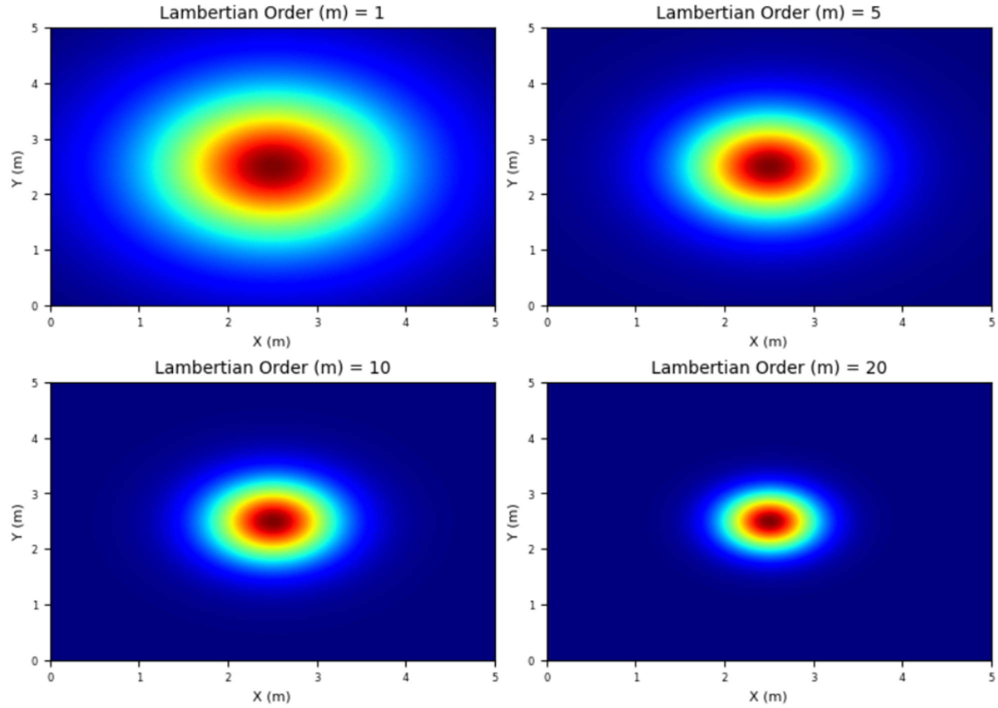

Figure 2.3: Lambertian radiation pattern

DC channel gain H can be written as [34]:

$$H = \begin{cases} \dfrac{(m+1)\,A}{2\pi\,d^2}\cos^m(\phi)\,\cos(\psi), & 0 \le \psi \le \Psi_\mathrm{c} \\ 0, & \text{otherwise} \end{cases} \tag{2.3}$$

where A is the PD's active area, ϕ is the LED's emission angle, ψ is the incidence angle at the PD, and Ψ_c denotes the field-of-view (FOV). The terms $\cos^m(\phi)$ and $\cos(\psi)$ capture the angular dependence of emission and detection, respectively. This model provides the foundation for analyzing received optical power, signal-to-noise ratio (SNR), and interference in indoor VLC systems.

2.1.3 Signal Model

Building on the channel gain H from (2.3), the received optical power P_r at the PD is

$$P_r = P_t \times H$$

where P_t is the LED's transmitted power. In the presence of shot and thermal noise, the total received signal can be expressed as

$$y(t) \;=\; P_r\, s(t) + n(t)$$

where $s(t)$ is the modulated signal (e.g., ADO-OFDM), and $n(t)$ is the additive white Gaussian noise (AWGN) component.

Multi-user Scenario In a multi-user VLC system based on NOMA, each user k may have a distinct channel gain $H^{(k)}$, dictated by its distance and orientation relative to the LED. Thus, user k's received power is

$$P_r^{(k)} \;=\; P_t \;\times\; H^{(k)}$$

When stronger-channel users are allocated lower transmit power and weaker channel users are assigned higher power, SIC can be used on the receiver side to separate overlapping signals. The details of power allocation and interference handling will be discussed in later sections.

2.2 OFDM Techniques in VLC

OFDM has a long history of success in RF systems, where it mitigates ISI and improves spectral utilization [37, 38]. In recent years, its application in VLC has garnered growing attention, as LEDs can serve dual roles for both illumination and data transmission.

OFDM differs from conventional Frequency Division Multiplexing (FDM) or Wavelength Division Multiplexing (WDM) schemes in that its subcarriers overlap in frequency but remain orthogonal within each symbol duration. As illustrated in Figure 2.4 [4], this eliminates the need for wide guard bands and enhances spectral efficiency. Demodulation relies on the computationally efficient fast Fourier transform (FFT), obviating extensive analog filtering hardware.

When transitioning OFDM into the optical domain, however, additional considerations arise. LEDs used in VLC demand unipolar and typically real-valued signals, compelling modifications such as DCO-OFDM or ACO-OFDM. Moreover, the LED's limited linear region and the high peak-to-average power ratio (PAPR) of OFDM signals can introduce nonlinearity

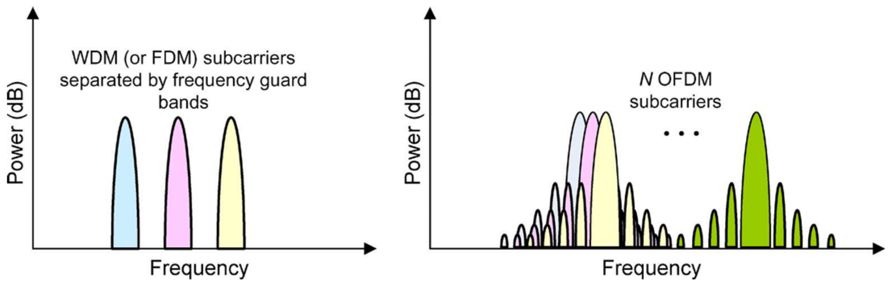

Figure 2.4: Illustration of OFDM subcarrier orthogonality [4].

distortion. These factors highlight the need to adapt or refine OFDM techniques for VLC, ensuring optimal power efficiency and data throughput under varying illumination conditions.

The following sections explore in detail how OFDM is adapted for VLC, examining different variants such as ACO-OFDM and DCO-OFDM, along with emerging methods that seek a balance between high spectral efficiency and low power consumption.

2.2.1 Evolution of OFDM in Optical Wireless

As shown in Fig. 2.5, the concept of OFDM dates back to early patents in the 1960s [37]. Through milestones in mobile communications, radio broadcasting, and optical applications, OFDM has become a robust solution for high-speed data transmission. Notably, the cyclic prefix (CP) was introduced in the 1980s to reduce inter-symbol interference Inter-Symbol Interference (ISI) [39], and forward error correction (FEC) further improved reliability in both RF and optical domains. The rise of Digital Signal Processing (DSP) techniques made it practical to adapt OFDM for LED based transmitters in VLC, where signals must be unipolar.

Benefits of OFDM in VLC Despite additional constraints such as the need for real, non-negative signals and the LED's limited linear region OFDM remains appealing for VLC. Its orthogonal subcarriers efficiently utilize the restricted modulation bandwidth, and FFT based implementation requires minimal analog filtering. OFDM resilience to ISI is also a key benefit in indoor VLC, where reflections can degrade signal quality. These strengths

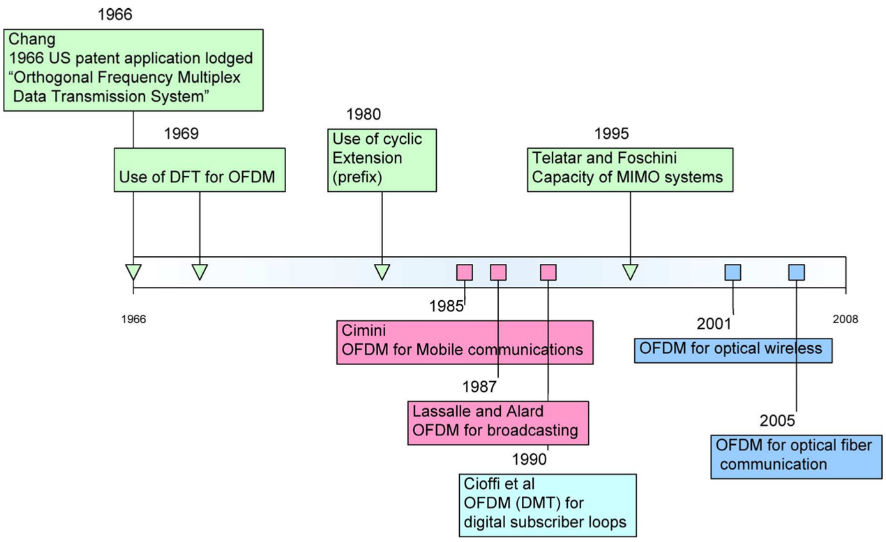

Figure 2.5: Historical progression of OFDM theory [4].

have motivated the development of specialized optical OFDM variants, such as ACO-OFDM and DCO-OFDM, to better accommodate the unipolar nature of LED based communication.

2.2.2 ACO-OFDM and DCO-OFDM

In optical intensity modulation, transmitting signals must be real and non negative. To meet this requirement, researchers have proposed specialized OFDM variants that differ in how they ensure unipolar waveforms:

- **ACO-OFDM** Data are transmitted only on the odd subcarriers, and the negative portion of the waveform is clipped at zero, producing a unipolar output. This design lowers power usage but reduces spectral efficiency, as only half of the subcarriers are utilized (see Fig. 2.6).

- **DCO-OFDM** A DC offset is added to shift the waveform above zero, enabling data transmission on both even and odd subcarriers. While this expands spectral efficiency, it also increases power consumption due to the higher bias level (see Fig. 2.7).

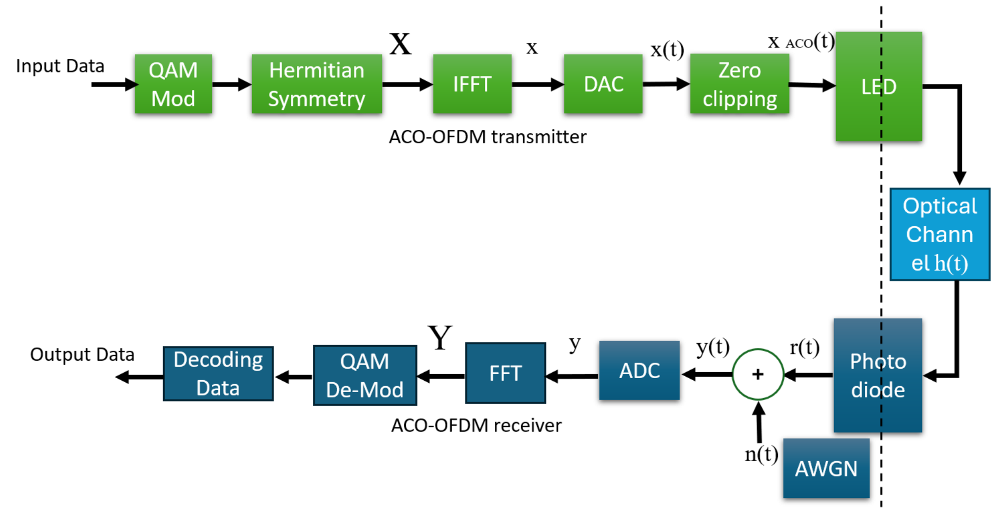

Figure 2.6: Illustration of ACO-OFDM

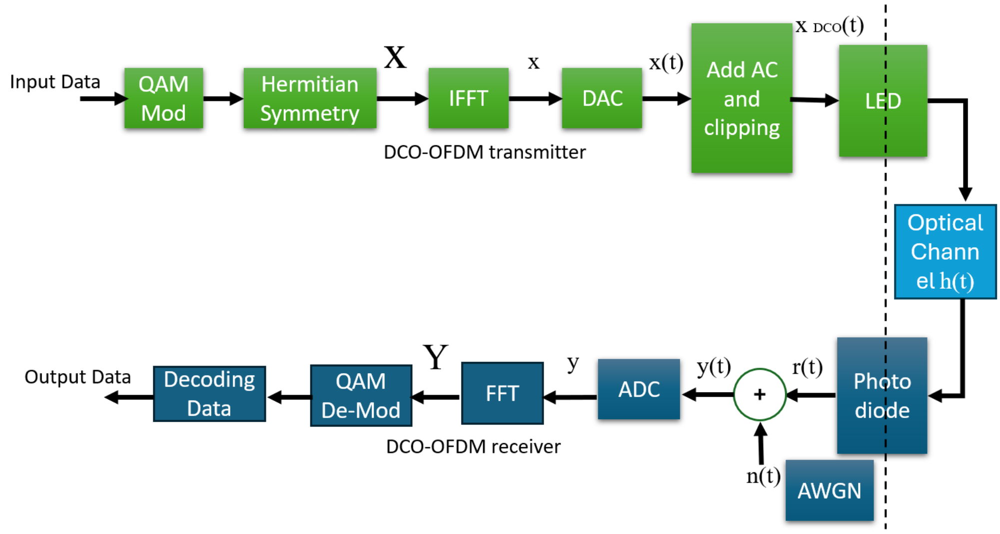

Figure 2.7: Illustration of DCO-OFDM

2.2.3 Challenges of OFDM in VLC

Despite OFDM's known advantages in bandwidth efficiency, LED nonlinearity, clipping noise, and high Peak-to-Average Power Ratio (PAPR) still pose significant obstacles. Existing approaches, such as pre distortion, companding, or iterative clipping and filtering, aim to mitigate these issues. More advanced solutions may integrate these methods with multiple-access schemes (e.g., NOMA) to further improve efficiency and robustness under multi-user conditions.

2.3 NOMA in VLC

NOMA is a key technique in VLC systems, enabling efficient multi-user communication by utilizing power domain multiplexing. Unlike traditional orthogonal methods, NOMA allows multiple users to share the same time-frequency resources by assigning different power levels based on their channel conditions (see Figure 2.8 and Figure 2.9).

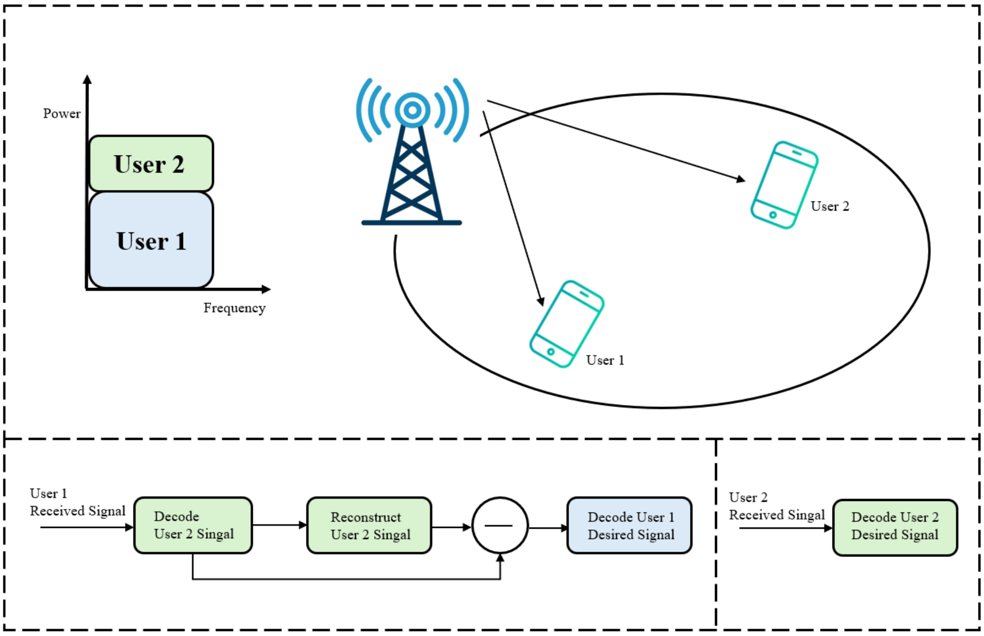

Figure 2.8: Conceptual diagram of NOMA

Stronger users (closer to the LED) are allocated lower power, while weaker users (farther from the LED) receive higher power to ensure fairness and meet quality-of-service requirements. SIC is used at the receiver to decode signals, starting with the strongest signal, and progressively subtracting it to retrieve weaker signals.(see Figure 2.10)

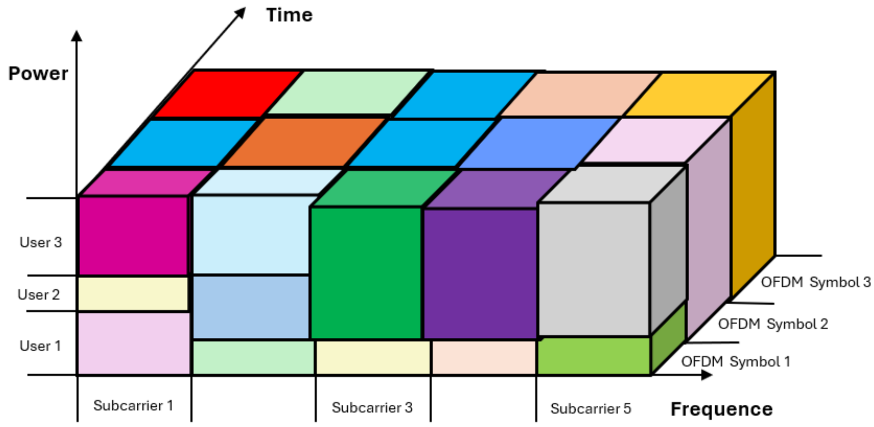

Figure 2.9: Conceptual diagram of NOMA

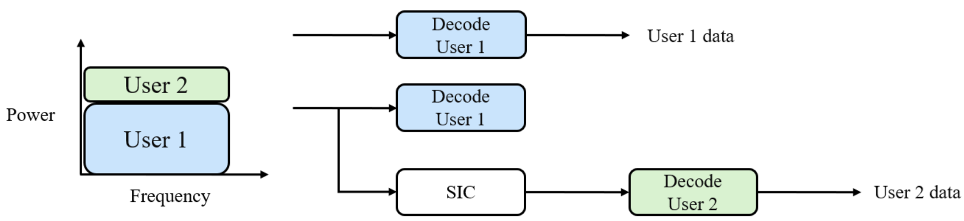

Figure 2.10: Conceptual diagram of NOMA SIC

The integration of NOMA in VLC enhances spectral efficiency and user connectivity, making it ideal for scenarios with heterogeneous user demands, such as smart homes, and smart factory systems. It also addresses the high user density and bandwidth limitations of VLC. However, challenges such as accurate power allocation, managing inter-user interference, and ensuring efficient SIC in practical VLC channels must be addressed.

NOMA adaptability and ability to support massive connectivity make it a critical component in advancing. VLC systems, particularly in multi-user environments, require dynamic resource allocation and high efficiency. Its combination with VLC ensures enhanced system capacity and user fairness, paving the way for next-generation wireless communication systems.

2.3.1 Multi-User NOMA for VLC

When adopting NOMA for more than two users in a VLC system, power-domain multiplexing and SIC can significantly improve throughput and spectrum efficiency. For example, in a four-user scenario (Users 1, 2, 3, and 4), each user's signal is superimposed at a specific power level in the same frequency band, and then decoded in descending order of power via SIC. Typically, weaker channel users receive higher transmit power to ensure reliable detection, while stronger channel users are assigned lower power to reduce interference. This approach outperforms orthogonal schemes by exploiting overlapping signals in the power domain, thereby addressing the near–far issue and enhancing fairness across different channel conditions. Nonetheless, scaling to larger user populations increases complexity in power allocation and user grouping and may exacerbate LED related constraints such as non linearity and high peak-to-average power ratios. As the network grows, advanced signal processing and resource management methods are required to maintain system performance and energy efficiency in multi-user VLC deployments.

2.3.2 Power Allocation and User Grouping

Effective power allocation is critical for boosting performance in NOMA VLC systems, and various user grouping approaches can further improve fairness and spectral utilization. Recent studies propose different strategies to address challenges such as channel disparity, energy efficiency, and multi-lamp deployments:

Minimizing Channel Gain Differences [5] Figure 2.11 illustrates a grouping scheme based on Maximizing Channel Gain Difference (MCGD). In this method, users are sorted in ascending order of their channel gains and then assigned into different subsets, with the goal of maximizing the channel-gain disparity among users within each group. By pairing users with relatively strong and weak channels together, power allocation can more easily exploit these large channel-gain differences—particularly useful in NOMA systems. However, MCGD suffers from inflexibility—it uses a fixed grouping approach that may become suboptimal under dynamic conditions, and it may also limit the full benefits of NOMA if other constraints (e.g., variable traffic loads or higher-order modulation) are not accounted for.

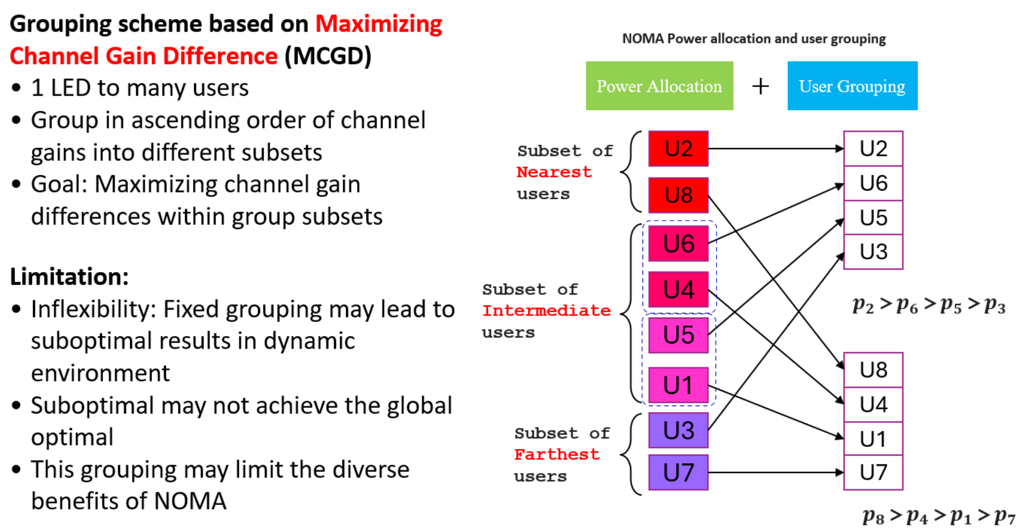

Figure 2.11: Grouping scheme based on maximizing channel gain difference [5].

Energy Efficiency Maximization [6] Another approach focuses on energy efficiency (EE), shown in Figure 2.12. By applying fractional programming techniques, the non-convex power allocation problem is transformed into a solvable, convex form under constraints such as minimum data rate, maximum LED power, and SIC requirements. Iterative algorithms then adjust transmit power to optimize EE, demonstrating that NOMA based VLC outperforms traditional orthogonal multiple access (OMA) systems, particularly when the number of LEDs or the power multiplexing factor grows. Nevertheless, this method could become computationally intensive in highly dynamic scenarios with many users, and it may not fully capture the effects of LED nonlinearity or intricate user-grouping constraints.

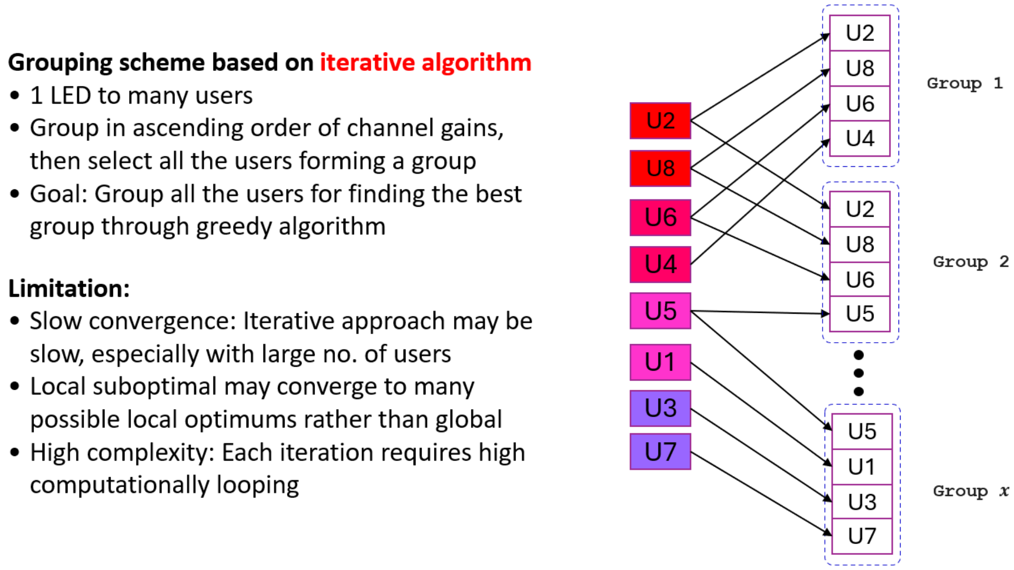

Figure 2.12: Grouping scheme based on iterative algorithm [6].

Multi-Lamp Resource Allocation [7] For more complex indoor deployments, Reference [7] extends power allocation to multi-lamp, multi-user scenarios (see Figure 2.13). In addition to pairing strong and weak users, the framework integrates subcarrier allocation to maximize throughput while preserving fairness. By managing resource allocation across multiple LED transmitters, this method supports large scale VLC networks and diverse user distributions. One limitation, however it is that it can introduce elevated complexity in coordinating subcarriers and power levels across numerous lamps, potentially requiring advanced signal processing techniques to maintain efficiency.

These approaches highlight different objectives channel disparity reduction, energy efficiency, and multi lamp coordination but each addresses only

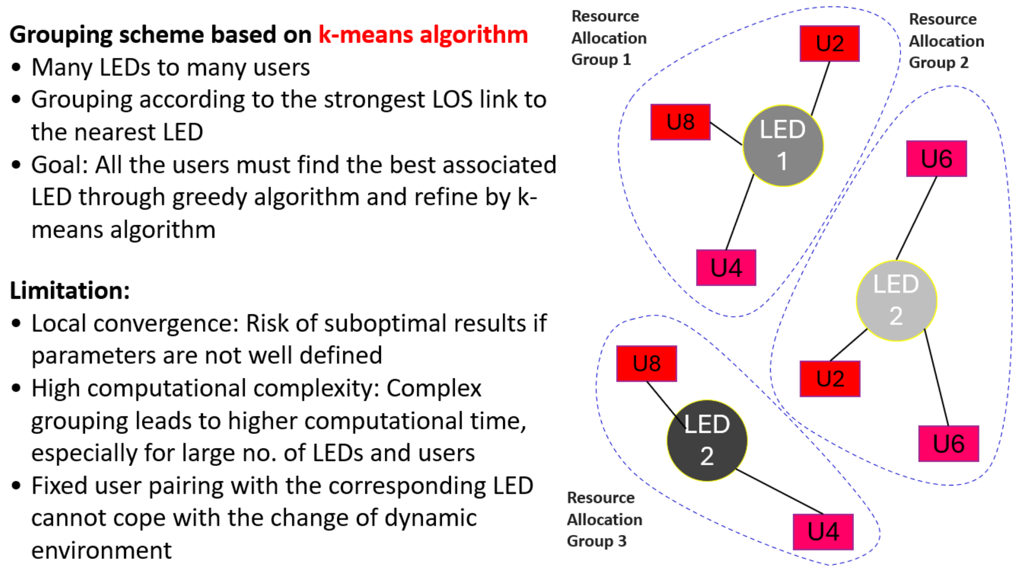

Figure 2.13: Grouping scheme based on k-means algorithm [7].

a subset of the broader challenges in NOMA VLC. As user counts increase and optical constraints become more stringent, issues such as LED nonlinearity, high peak-to-average power ratios, and complex grouping requirements must be resolved simultaneously. By grouping users intelligently and adapting power levels, NOMA VLC systems can better manage heterogeneous channel conditions, improve fairness, and boost spectral efficiency; however, more comprehensive solutions are needed to integrate higher-order modulation schemes, sophisticated LED models, and dynamic user distributions.

The insights gained from these strategies set the stage for the proposed model in Chapter 3, where an advanced user grouping and power control method is integrated into an ADO-OFDM framework to address both spectral and energy efficiency in multi-user VLC. This combined approach aims to overcome the limitations of existing studies, offering a more robust and scalable solution for dense indoor environments.

2.4 Summary

This chapter presented essential background on visible light communication (VLC), beginning with the optical channel model and the constraints of intensity modulation in indoor environments. It then examined key OFDM-based techniques, including ACO-OFDM and DCO-OFDM, emphasizing how their unipolar signal requirements differ from traditional RF OFDM. Next, the chapter explored NOMA principles within VLC, underscoring the potential for improved spectral efficiency and multi-user support through power domain multiplexing. Various power allocation and user grouping strategies were also reviewed, highlighting both their strengths and notable gaps particularly in handling dynamic channels, LED nonlinearity, and large-scale deployments.

Building on these foundational insights, the next chapter proposes an advanced ADO-OFDM NOMA framework designed to address the challenges identified here. By combining ACO-OFDM and DCO-OFDM with adaptive user grouping and power control, the proposed solution aims to enhance system performance, fairness, and scalability in multi-user VLC networks.

Chapter 3

Proposed NOMA VLC Systems with Grouping Scheme

This chapter presents the proposed NOMA VLC systems and its associated grouping scheme, highlighting the novel power allocation algorithms developed in this work. We begin by describing the proposed ADO-OFDM NOMA approach for VLC and then extend it to MCGAD-NOMA. Finally, we discuss the grouping scheme algorithm, outlining its initialization, optimization, and selection phases. The detailed principles and relevant design considerations for each component are provided in the following sections.

3.1 Proposed NOMA Systems for VLC

To enhance multi-user capacity and power efficiency in VLC systems, we adopt an indoor NOMA-VLC system, as illustrated in Fig. 3.1. At the transmitter side, the baseband signal first undergoes modulation (e.g., ACO-OFDM or DCO-OFDM) and is then superimposed with a DC bias. The LED transmitter not only provides illumination but also carries the backbone data via intensity modulation. Specifically, the LED's intensity is varied according to the input electrical signal, thus embedding information in the optical domain.

On the receiver side, a photodiode utilizes DD to retrieve the optical carrier wave and extract the transmitted signal [35]. After amplification, filtering, and demodulation, the original data can be recovered. Suppose all

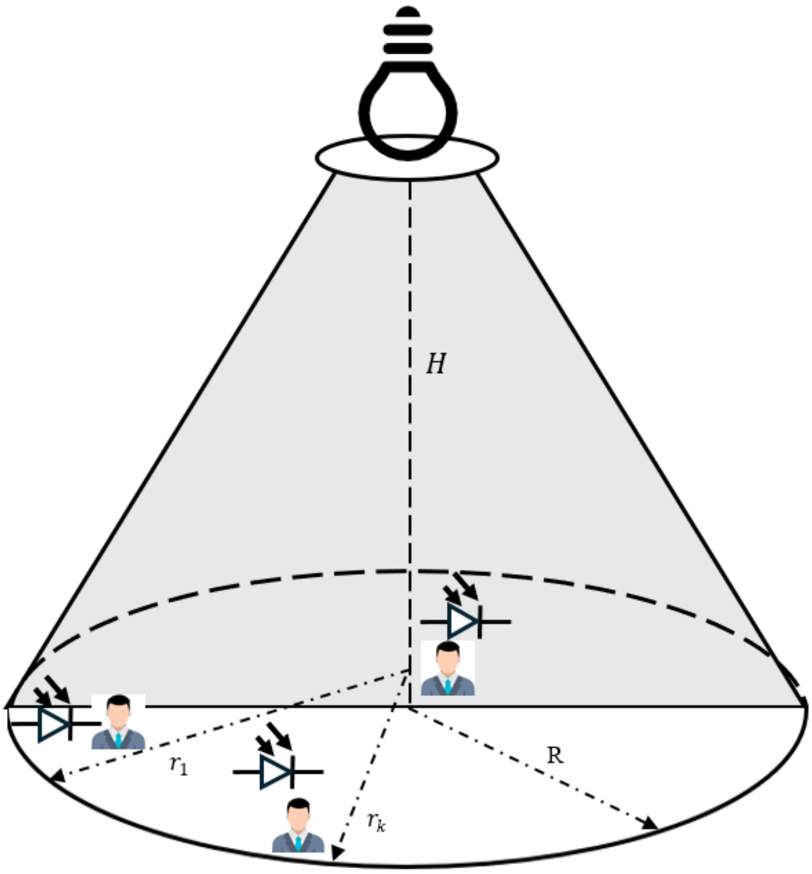

Figure 3.1: Diagram of an indoor NOMA-VLC system

users' DC channel gains follow the ordering

$$h_1 \leq \cdots \leq h_k \leq \cdots \leq h_M$$

where h_k denotes the k-th user's DC channel gain. Consequently, the horizontal distances from the LED to each user satisfy

$$r_1 \geq \cdots \geq r_k \geq \cdots \geq r_M$$

, indicating that users closer to the LED typically achieve higher channel gains than those farther away.

Building upon fundamental insights from a simpler two-user case, which is based on ACO-OFDM and DCO-OFDM (jointly referred to as ADO-OFDM) this design can be extended to multiple users under NOMA VLC. By intelligently grouping users with varying gains, the system superimposes signals in the power domain at the LED and harnesses SIC at the PD side, thereby accommodating larger user sets under diverse traffic loads. This paper further introduces an advanced *MCGAD NOMA* approach, enabling flexible multi-user grouping strategies and improved overall throughput.

3.2 ADO-OFDM NOMA

This section introduces ACO-OFDM and DCO-OFDM, two prominent modulation techniques for optical wireless systems that can be combined into ADO-OFDM, thereby offering a robust, high capacity technique when integrated with NOMA principles (see Figure 3.2).

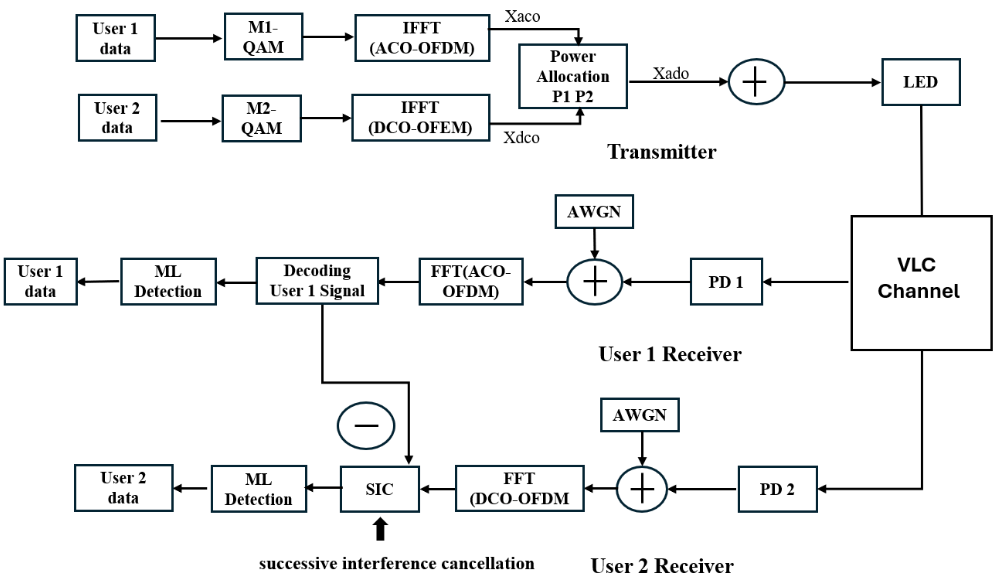

Figure 3.2: Two-user ADO-OFDM NOMA for VLC

ADO-OFDM NOMA stands out as a promising strategy to increase capacity and performance in VLC systems. By merging ACO-OFDM power efficiency with DCO-OFDM comprehensive utilization of the amplitude range and overlaying multiple users via NOMA power-domain multiplexing, this approach significantly enhances spectral efficiency, user fairness and robustness to interference. Despite challenges related to power allocation, receiver complexity, and the inherent variability of indoor VLC channels, ongoing research continues to refine ADO-OFDM NOMA techniques (see Figure 3.3).

3.2.1 ADO-OFDM NOMA Transmitter

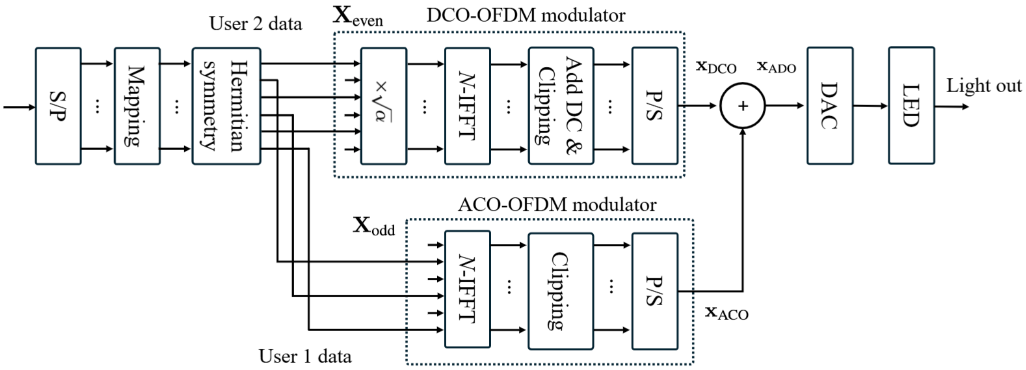

Figure 3.3: Proposed ADO-OFDM NOMA transmitter

Figure 3.3 shows the structure of the proposed ADO-OFDM transmitter used for supporting NOMA transmission. In this structure, the data transmitted by user 1, located relatively far from the LED transmitter, is modulated onto the ACO-OFDM signal component, while the data transmitted by user 2, located relatively close to the LED, is modulated onto the DCO-OFDM signal component.

To generate the ACO-OFDM component, the binary data sequence intended for user 1 is initially mapped onto a group of QAM symbols. These QAM symbols are then loaded onto the odd subcarriers of the OFDM signal, while the even subcarriers remain unused and are loaded with zeros. Therefore, the frequency domain QAM values sent into IFFT are given by

$$\mathbf{X}_{\text{ACO}} = [0, X_1, 0, X_3, \ldots, X_k \ldots, 0, X_{N-1}] \tag{3.1}$$

where X_k is the QAM symbol loaded on the kth subcarrier and N is the overall number of subcarriers. Moreover, the values within $\mathbf{X}_{\text{ACO}}$ are constrained to have Hermitian symmetry which is defined as

$$X_k = X^*_{N-k}, 0 < k < \tfrac{N}{2} \tag{3.2}$$

Consequently, the time domain sequence obtained using IFFT is as follows

$$x_{\text{ACO},n} = \frac{1}{\sqrt{N}} \sum_{k=0}^{N-1} X_{\text{ACO},k} \exp\left(\frac{j2\pi kn}{N}\right), \tag{3.3}$$

for $n = 0, 1, ..., N-1$, only contains real values. In ACO-OFDM, since only odd subcarriers are loaded with data, $\mathbf{x}_{\text{ACO}} = [x_{\text{ACO},0}, x_{\text{ACO},1}, ..., x_{\text{ACO},N-1}]$ has the anti-symmetry property as

$$x_{\text{ACO},n} = -x_{\text{ACO},n+\frac{N}{2}}, \tag{3.4}$$

for $0 < n < \frac{N}{2}$. Next, $\mathbf{x}_{\text{ACO}} = [x_{\text{ACO},0}, x_{\text{ACO},1}, ...x_{\text{ACO},n}, ..., x_{\text{ACO},N-1}]$ is clipped at its zero level as

$$x_{\text{ACO},n}^{\text{user 1}} = \begin{cases} x_{\text{ACO},n}, & \text{if } x_n > 0 \\ 0, & \text{if } x_n \leq 0 \end{cases} \tag{3.5}$$

to generate a unipolar signal which is suitable for an IM/DD system. Alternatively, the clipping operation shown in (3.5) can be given by

$$x_{\text{ACO},n}^{\text{user 1}} = \frac{1}{2}(x_{\text{ACO},n} + |x_{\text{ACO},n}|). \tag{3.6}$$

In ACO-OFDM, since $x_{\text{ACO},n}$ is anti-symmetrical, the clipping operation only attenuates the amplitude of the QAM symbols loaded on the odd subcarriers by half, which is $\frac{1}{2}x_{\text{ACO},n}$. The clipping noise, $\frac{1}{2}|x_{\text{ACO},n}|$, only falls on the even subcarriers and does not distort the QAM symbols carried on the odd subcarriers.

To generate the DCO-OFDM signal component that carries the data transmitted for user 2, the mapped QAM symbols are placed on the even subcarriers. Unlike conventional ADO-OFDM, a power allocation coefficient, α is introduced to adjust the power of the DCO-OFDM component relative to the ACO-OFDM component. This adjustment aims to balance the performance between different users in a NOMA system where two users have different channel conditions. In this case, the QAM values are given by

$$\mathbf{X}_{\text{DCO}} = \sqrt{\alpha}[X_0, 0, X_2, 0, \ldots, X_{N-2}, 0]. \tag{3.7}$$

Next, similar to (3.3), $\mathbf{X}_{\text{DCO}}$ is transformed to a time domain sequence, $\mathbf{x}_{\text{DCO}} = [x_{\text{DCO},0}, x_{\text{DCO},1}, ..., x_{\text{DCO},N-1}]$, using IFFT. Then, a DC bias, B_{DC} is added on to $x_{\text{DCO},n}$. The level of B_{DC} is set relatively to the standard deviation of the $x_{\text{DCO},n}$ using

$$B_{\text{DC}} = \mu\sqrt{E(x_{\text{DCO},n}^2)} \tag{3.8}$$

and it is defined in dB as $10\log_{10}(\mu^2+1)$ dB [40]. Next, similar to (3.5), the signal is clipped at its zero level to obtain a unipolar signal, $x_{\mathrm{DCO},n}^{\mathrm{user}\ 2}$ which carries the data transmitted for user 2.

Then, the DCO-OFDM signal and the ACO-OFDM signal are superimposed in the time domain as

$$x_{\mathrm{ADO},n} = x_{\mathrm{ACO},n}^{\mathrm{user}\ 1} + x_{\mathrm{DCO},n}^{\mathrm{user}\ 2}. \tag{3.9}$$

Finally, $x_{\mathrm{ADO},n}$ is sent into a digital-to-analog converter (DAC) to generate an analogy electrical signal, $x_{\mathrm{ADO}}(t)$, which is used to directly drive the LED transmitter.

3.2.2 ADO-OFDM NOMA Receiver

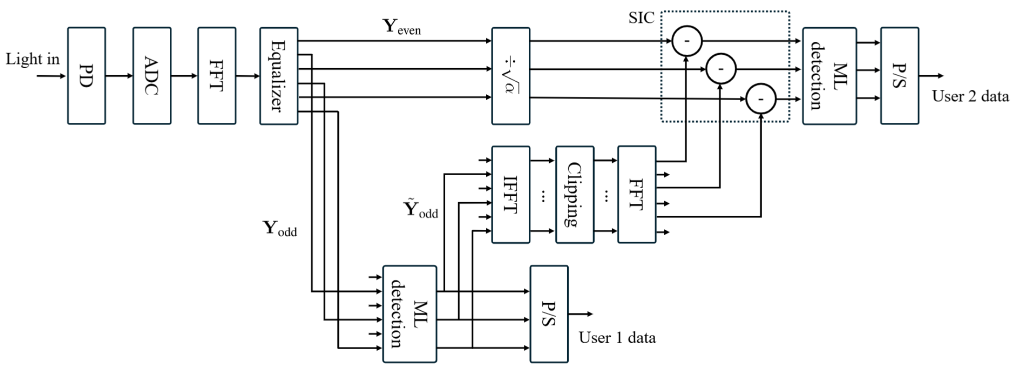

Figure 3.4: Proposed ADO-OFDM NOMA receiver

Figure 3.4 shows the structure of the proposed ADO-OFDM receiver for two users that needs to be demodulated using different approaches. At the receiver of user 1, $y(t)$ is first sent into an ADC to obtain y_m. Then, channel equalization is performed using

$$\bar{y}_m = h^{-1}y_m. \tag{3.10}$$

For the sake of simplicity, we only consider the optical channel gain. In a practical transmission, the overall channel response is usually not flat due to the frequency response of the LED and/or the photodiode. In such cases, channel equalization would be implemented in the frequency domain using a group of single-tap equalizers.

Next, $\bar{y}_m$ is transformed into the frequency domain using

$$Y_k = \frac{1}{\sqrt{N}} \sum_{n=0}^{N-1} \bar{y}_m \exp\left(-\frac{j2\pi kn}{N}\right) \tag{3.11}$$

for $k = 0, 1, \ldots, N-1$. Since the data transmitted for user 1 is modulated onto the QAM symbols carried on the odd subcarriers, the

$$\mathbf{Y}_{\text{odd}} = [0, Y_1, 0, Y_3, \ldots, 0, Y_{N-1}] \tag{3.12}$$

are sent into an ML demodulator to estimate the transmitted QAM symbols, $\tilde{\mathbf{Y}}_{\text{odd}}$ using

$$\tilde{Y}_{\text{odd},k} = \underset{X \in \mathbb{Z}_{M\text{-QAM}}}{\operatorname{argmin}} \left\| 2\, Y_{\text{odd},k} - X \right\|, \tag{3.13}$$

where $\mathbb{Z}_{M\text{-QAM}}$ denotes the M-QAM constellation space, and M is the QAM constellation size. Finally, $\mathbf{Y}_{\text{odd}}$ is de-mapped into a binary sequence to recover the transmitted data for user 1.

In the case of user 2, its signal demodulation is a SIC process. First, identical to the above steps, the QAM symbols transmitted for user 1 are estimated. Then, $\mathbf{Y}_{\text{odd}}$ is transformed back to the time domain using Inverse Fast Fourier Transform (IFFT) and then clipped at its zero level. In this case, the clipping noise that falls on the even subcarriers, $\tilde{\mathbf{Y}}_{\text{even,CN}}$, can be estimated. Next, the even subcarriers of

$$\mathbf{Y}_{\text{even}} = [Y_0, 0, Y_2, \ldots, Y_{N-2}, 0] \tag{3.14}$$

are obtained. Then, the clipping noise from the ACO-OFDM signal component is removed from $\mathbf{Y}_{\text{even}}$ using

$$\tilde{\mathbf{Y}}_{\text{even}} = \frac{1}{\sqrt{\alpha}} \left(\mathbf{Y}_{\text{even}} - \tilde{\mathbf{Y}}_{\text{even,CN}} \right). \tag{3.15}$$

Finally, each of the QAM symbols within $\mathbf{Y}_{\text{even}}$ is sent into an ML demodulator to recover the data transmitted to user 2.

3.3 MCGAD NOMA

In practice, VLC networks often experience varying traffic loads and changing numbers of active users. To handle such dynamic conditions, we propose an

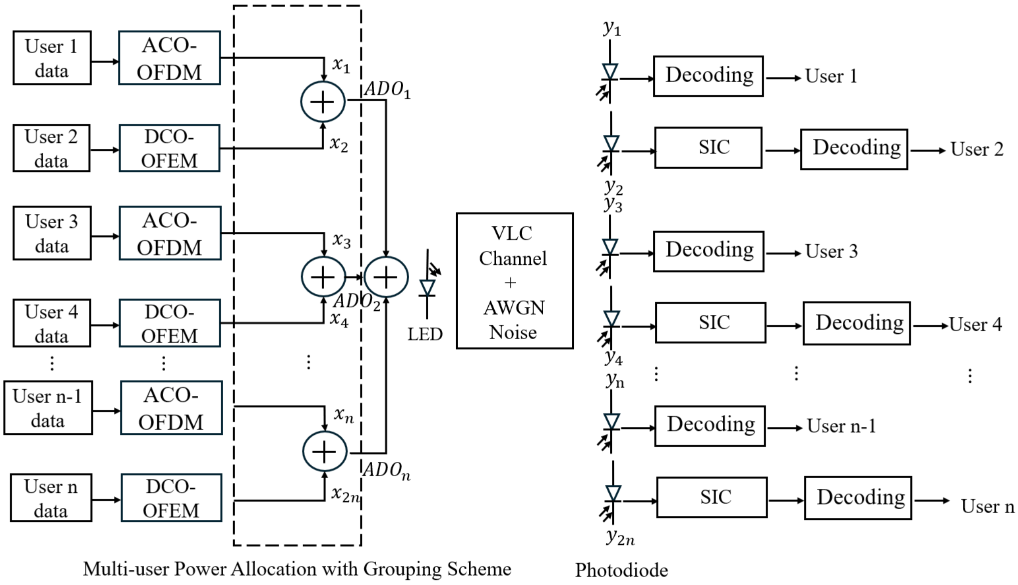

Figure 3.5: Proposed ADO-OFDM NOMA for multi-user VLC

integrated *MCGAD NOMA* technique that unifies two set of two-user ADO-OFDM NOMA approach to achieve higher capacity in multi-user NOMA VLC systems.

Figure 3.6 illustrates the overall idea: Multiple users are grouped into pairs, each pair forming a two-user ADO-NOMA block, and then these blocks are superimposed in the power domain.

Specifically, Let $n \geq 4$ be the total number of users, with $k \geq 2$ such that $n = 2k$. The variable n represents the overall number of users to be grouped, while k indicates the number of *two-user* ADO pairs.

When forming these ADO pairs, the multi-user transmitted signal can be constructed by combining each two-user ADO block in the power domain. For example, if we denote the multi-user ADO signal for the (n, k)-th grouping by $S^{\text{ado}}_{(n,k)}(t)$, one possible form is

$$S^{\text{ado}}_{(n,k)}(t) \;=\; \sqrt{\frac{p_{n-3}}{p_{n-2}}}\, x^{\text{ado}}_{k-1}(t) \;+\; \sqrt{\frac{p_{n-1}}{p_n}}\, x^{\text{ado}}_{k}(t), \tag{3.16}$$

where p_i are power-allocation coefficients for user i, and $x^{\text{ado}}_j(t)$ represents the ADO waveform corresponding to the j-th two-user pair. As a concrete

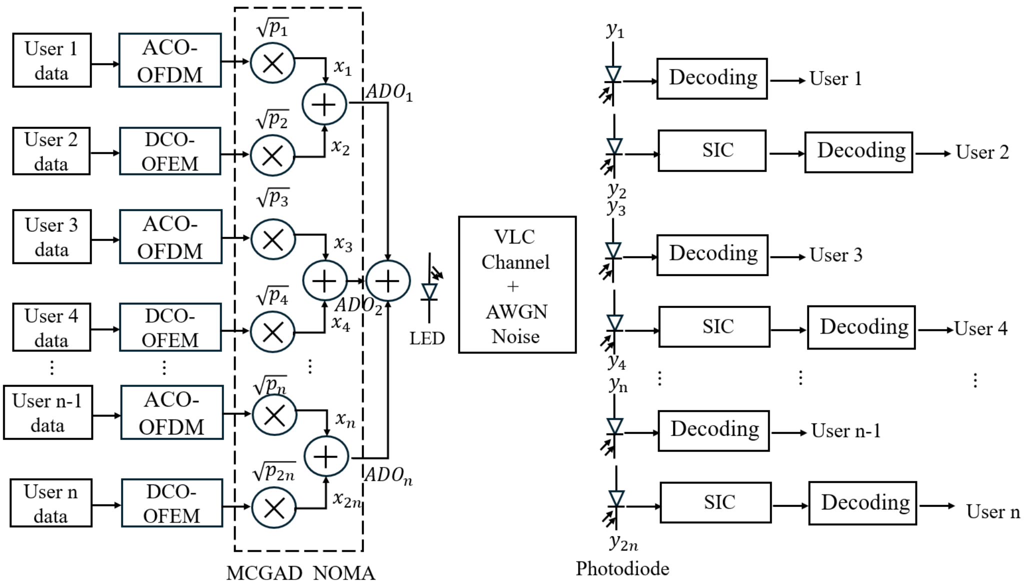

Figure 3.6: Proposed MCGAD NOMA for multi-user VLC

example, when $n = 4$ and $k = 2$, this becomes

$$S^{\text{ado}}_{(4,2)}(t) \; = \; \sqrt{\frac{p_1}{p_2}}\, x^{\text{ado}}_1(t) \; + \; \sqrt{\frac{p_3}{p_4}}\, x^{\text{ado}}_2(t). \tag{3.17}$$

Within each two-user ADO block, the signal can further be split according to

$$x^{\text{ado}}_{(n-k)}(t) \; = \; \sqrt{p_{n-1}}\, x_{\,n-1}(t) \; + \; \sqrt{p_n}\, x_{\,n}(t), \tag{3.18}$$

where $x_{\,n-1}(t)$ and $x_{\,n}(t)$ denote the baseband signals of user $n-1$ and user n. For instance, if $n = 4$ and $k = 2$, then

$$x^{\text{ado}}_2(t) \; = \; \sqrt{p_3}\, x_3(t) \; + \; \sqrt{p_4}\, x_4(t), \tag{3.19}$$

and in the simpler case where $n = 2$ and $k = 1$,

$$x^{\text{ado}}_1(t) \; = \; \sqrt{p_1}\, x_1(t) \; + \; \sqrt{p_2}\, x_2(t). \tag{3.20}$$

Here, $x_1(t)$, $x_2(t)$, $x_3(t)$, and $x_4(t)$ indicate transmitted baseband signals of user 1, user 2, user 3, and user 4, respectively, while p_1, p_2, p_3, and p_4 are the corresponding power-allocation coefficients.

The total transmit power allocated to each ADO block can be expressed as

$$p_T \; = \; \sum_{i=1}^{k} p^{\text{ado}}_i, \tag{3.21}$$

where p_i^{ado} denotes the overall power assigned to the i-th ADO two-user pair. For a four-user example with two ADO pairs, one might write:

$$s_1^{\mathrm{ado}}(t) \;=\; \sqrt{p_1}\, x_1(t) \;+\; \sqrt{p_2}\, x_2(t), \quad s_2^{\mathrm{ado}}(t) \;=\; \sqrt{p_3}\, x_3(t) \;+\; \sqrt{p_4}\, x_4(t), \tag{3.22}$$

so that $s_1^{\mathrm{ado}}(t)$ and $s_2^{\mathrm{ado}}(t)$ represent two ADO-OFDM superposed signals within the power domain.

Additional ratios are introduced to manage how power is partitioned among these blocks or within each ADO sub-layer. For instance,

$$\alpha \;=\; \frac{p_n}{p_{n-1}}, \qquad \beta \;=\; \frac{p_k^{\mathrm{ado}}}{p_{k-1}^{\mathrm{ado}}},$$

may denote power ratios between the DCO-OFDM and ACO-OFDM components, or between different ADO two-user groups. These parameters allow flexible allocation: for example, α could split the DCO-OFDM power from the ACO-OFDM share, while β controls the relative power of two adjacent ADO groups. If user 1 and user 2 jointly occupy one ADO block, the power might be set to $\beta\, p_1^{\mathrm{ado}}$ for that block, whereas users 3 and 4 would then share $(1-\beta)\, p_2^{\mathrm{ado}}$. Such tunable partitioning ensures that users with weaker channels (or higher data-rate requirements) can be appropriately boosted.

Overall, this MCGAD NOMA structure offers a hybrid strategy that seamlessly transitions between two-user ADO and larger four-user (or higher) NOMA groupings. By adjusting each pair's power coefficients $\{p_i^{\mathrm{ado}}\}$, as well as the ratios α and β, the system accommodates varying traffic demands and channel conditions. In doing so, MCGAD NOMA can maximize both spectral efficiency and fairness in VLC networks, without resorting to entirely separate hardware paths for ACO-OFDM and DCO-OFDM. This integrated approach provides a robust, scalable solution for next-generation optical wireless systems.

3.4 Grouping Scheme

In this section, we introduce our proposed grouping scheme algorithm Figure 3.9 for multi-user VLC networks. Figure 3.10 offers an overview of its three core phases: *Initialization*, *Optimization*, and *Selection*. The objective is to cluster users effectively according to their channel gains, allocate power in a way that balances throughput and fairness, and refine these decisions iteratively to adapt to network changes.

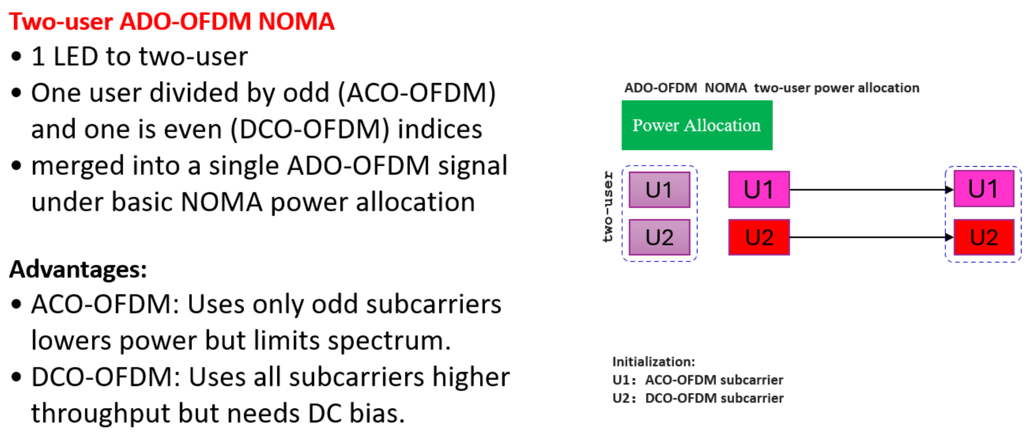

Figure 3.7: Proposed grouping scheme of ADO-OFDM NOMA for two-user VLC

During the Initialization phase, each user's channel gain $\{h_1, h_2, \ldots, h_N\}$ is measured, for instance, via pilot signals or feedback. A preliminary grouping is then formed based on these gains (e.g., the MCGAD principle pairs or clusters users to minimizing channel disparity). An initial power allocation $\mathbf{p}$ is assigned to each group. Algorithm 1 outlines the high-level steps of this basic setup, covering user sorting, odd/even subcarrier assignment (ACO/DCO), and the creation of initial ADO-NOMA blocks.

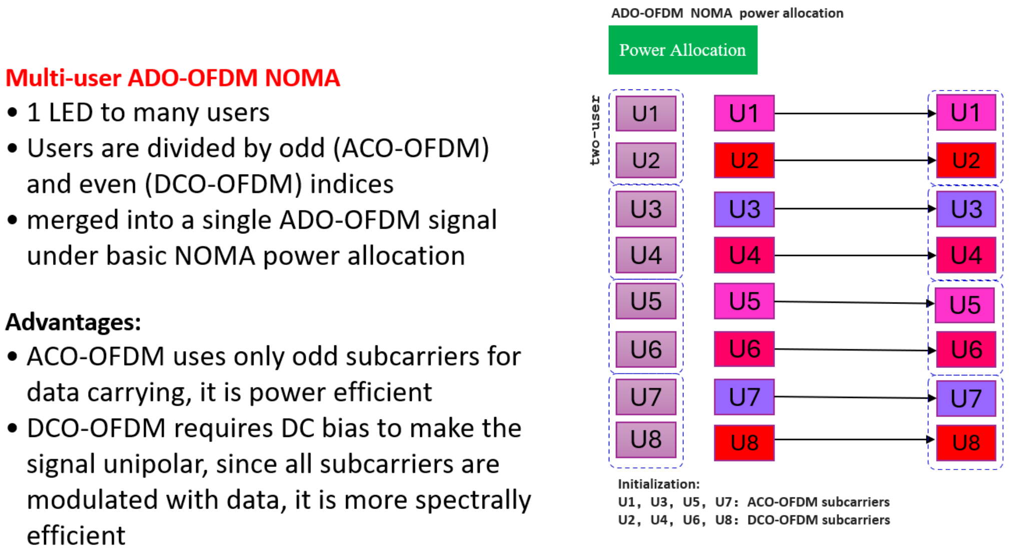

Figure 3.8: Proposed grouping scheme of ADO-OFDM NOMA for multi-user VLC

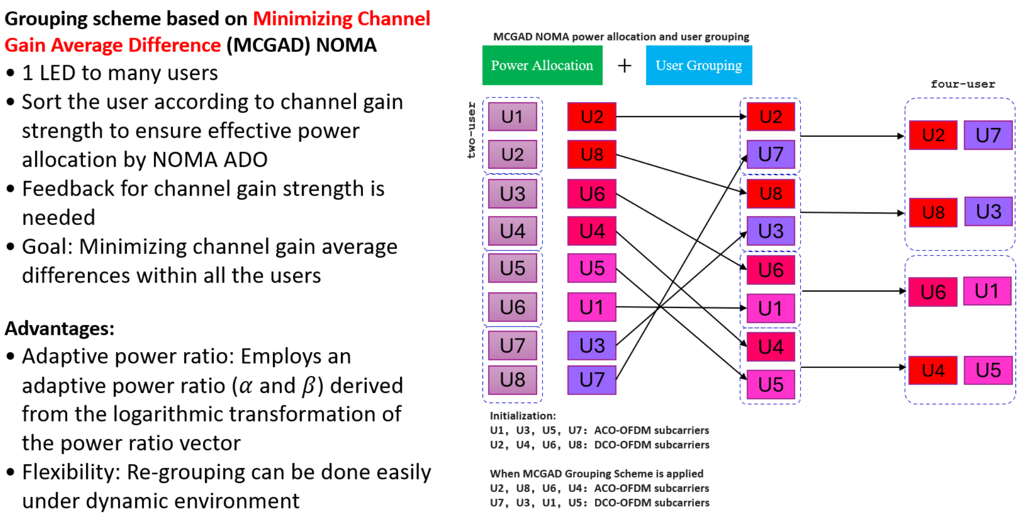

Figure 3.9: Proposed grouping scheme for MCGAD NOMA for multi-user VLC

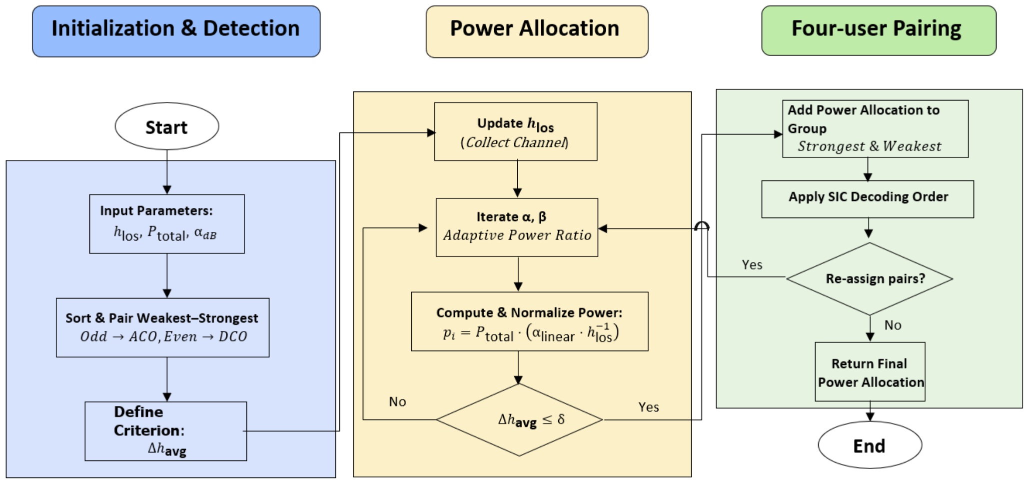

Figure 3.10: Flowchart of power allocation and user grouping for MCGAD NOMA

3.4.1 Power Allocation and User Grouping Algorithm for ADO-OFDM NOMA

Algorithm 1

Definition:

Let N be the total number of users.
Let $h_{i,\text{LOS}}$ denote the Lambertian (line-of-sight) channel gain for user i, computed via the Lambertian propagation model.
Let P_{total} be the total transmit power budget, and let α and β be power ratios for ADO combinations.

Stage 1: Initialization

1: **Input:** N, P_{total}, $\{h_{i,\text{LOS}}\}_{i=1}^{N}$, desired power ratio ranges for (α, β)
2: **Compute** $h_{i,\text{LOS}}$ for each user i using Lambertian model (e.g., via (2.1)) ▷ LOS channel gains
3: **Sort** users by ascending channel gain:

$$h_{(1),\text{LOS}} \leq h_{(2),\text{LOS}} \leq \cdots \leq h_{(N),\text{LOS}}$$

▷ Parentheses indicate sorted indices
4: **Assign Odd/Even Subcarriers:** ▷ Grouping ACO and DCO

- Odd subcarriers → ACO–OFDM
- Even subcarriers → DCO–OFDM

Stage 2: Power Allocation

5: **Combine** ACO and DCO carriers to form ADO–OFDM subcarriers. Define a ratio $\alpha \in [\alpha_{\min}, \alpha_{\max}]$ to split power between different ADO subcarriers.
6: **Define** β as the ratio that balances the relative power between ACO and DCO parts for each ADO subcarrier.
7: **Iterate** over feasible pairs (α, β) to minimize some objective function, e.g. the difference among users' channel gains or the total BER:

$$\Delta h_{i,\text{LOS}} \quad \text{or} \quad \text{BER}_{\text{avg}}$$

8: **Compute Power Allocation:** For each user i, define

$$p_i \;=\; P_{\text{total}} \times f(\alpha, \beta, h_{i,\text{LOS}})$$

where $f(\cdot)$ is a function that normalizes total power under the chosen (α, β) pair. (One could apply $\sum_i p_i = P_{\text{total}}$.)

9: **Check Convergence:** If the optimization condition (e.g. Δh_{LOS} minimized or BER_{avg} below threshold) is satisfied, proceed; otherwise, adjust (α, β) and repeat.

Stage 3: User Pairing

10: **Apply SIC decoding order**: Decode strongest user first, weakest user last, or vice versa depending on ADO-OFDM NOMA approach.

11: **Store Final** (α, β)**,** p_i for each user. ▷ Allocate the computed power to each user's ADO subcarrier.

12: **Return** $\{\,(p_i)_{i=1}^{N},\ \alpha^*,\ \beta^*\}$ as the final power allocation.

3.4.2 Power Allocation and User Grouping Algorithm for MCGAD NOMA

Algorithm 2 Initialization & Detection

Definition:

Let N be the total number of users.
Let $\{h_{i,\mathrm{LOS}}\}_{i=1}^{N}$ be each user's LOS channel gain, and let P_{total} be the total transmit power budget.
Suppose ACO-OFDM for odd-indexed subcarriers and DCO-OFDM for even-indexed subcarriers, forming ADO blocks. The goal is to minimize the average channel-gain difference, denoted by Δh_{avg}, across all user pairs.

Initialization and Detection

1: **Input:** N, P_{total}, $\{h_{i,\mathrm{LOS}}\}$, tolerance ϵ for Δh_{avg}.

2: **Sort** the users by ascending channel gain:

$$h_{(1),\mathrm{LOS}} \;\le\; h_{(2),\mathrm{LOS}} \;\le\; \cdots \le\; h_{(N),\mathrm{LOS}}.$$

3: **Group into Pairs:** ▷ Make a pair for the weakest with the strongest one for $N = 2k$.

$$\text{Pair 1: } \Big(h_{(1),\mathrm{LOS}},\, h_{(N),\mathrm{LOS}}\Big), \quad \text{Pair 2: } \Big(h_{(2),\mathrm{LOS}},\, h_{(N-1),\mathrm{LOS}}\Big), \ldots$$

▷ Alternatively, group sequentially depending on MCGAD policy.

4: **Set** initial power allocation $p_i = P_{\mathrm{total}}/N$ for each user (or use a simple heuristic, e.g. more power to weaker users).

5: **Compute** initial average difference:

$$\Delta h_{\mathrm{avg}} \;=\; \frac{1}{k}\sum_{j=1}^{k}\Big|\, h_{(j),\mathrm{LOS}} \;-\; h_{(N-j+1),\mathrm{LOS}}\Big|.$$

Iterate or Pass to Algorithm 3

$\Delta h_{\mathrm{avg}} \le \delta$ If **no**, proceed to Algorithm 3. If **yes**, skip further adjustment.

6: **Return** initial grouping $\{(h_{(1),\mathrm{LOS}},\, h_{(N),\mathrm{LOS}}), \ldots\}$ and $\{p_i\}_{i=1}^{N}$.

Algorithm 3 Power Allocation and Four-user Pairing

Definition:

The goal is to reassign power allocation and finalize the four-user pairing.

Power Allocation

1: **Receive** feedback from each user regarding $h_{(i),\mathrm{LOS}}$ updates (if channel varies) and their QoS requirements (e.g., minimum data rate).

2: **Iterate over** candidate pairs (α, β) in the feasible domain (e.g., $\alpha \in [\alpha_{\min}, \alpha_{\max}]$, $\beta \in [\beta_{\min}, \beta_{\max}]$). ▷ See flowchart: "Iterate α, β."

3: **Compute** normalized power for each user i:

$$p_i \;\leftarrow\; P_{\text{total}} \times g\Big(\alpha, \beta, h_{i,\mathrm{LOS}}\Big),$$

where $g(\cdot)$ enforces $\sum_i p_i \leq P_{\text{total}}$ and accounts for grouping strategy (e.g., the *weakest* user in each pair might get higher power).

4: **Check Objective**: e.g.

$$\Delta h_{\text{avg}} \quad \text{or} \quad \mathrm{BER}_{\text{avg}}, \quad \text{throughput, etc.}$$

If improved, keep the updated (α, β); otherwise discard.

5: **Repeat** until no further improvement in objective or maximum iterations reached.

Four-user Pairing

6: **Set** the final power allocation $\{p_i\}$ based on the best (α, β) found above.

7: **Decide** on SIC decoding order: either strongest-first or weakest-first depending on ADO-OFDM NOMA approach.

8: **If** any ungrouped users remain (e.g. when N is odd or the channel matrix changes), re-group them by returning to **Algorithm 2** with updated channel feedback.

9: **Return** final grouping, power allocation $\{p_i\}_{i=1}^{N}$, and decoding order for each pair.

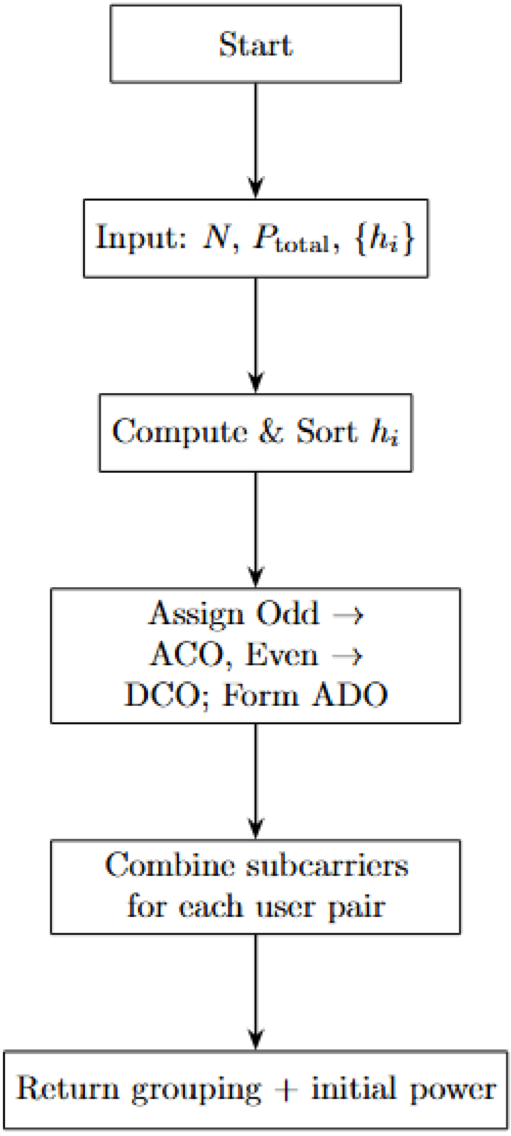

Figure 3.11: Flowchart of power allocation and user grouping algorithm for ADO-OFDM NOMA

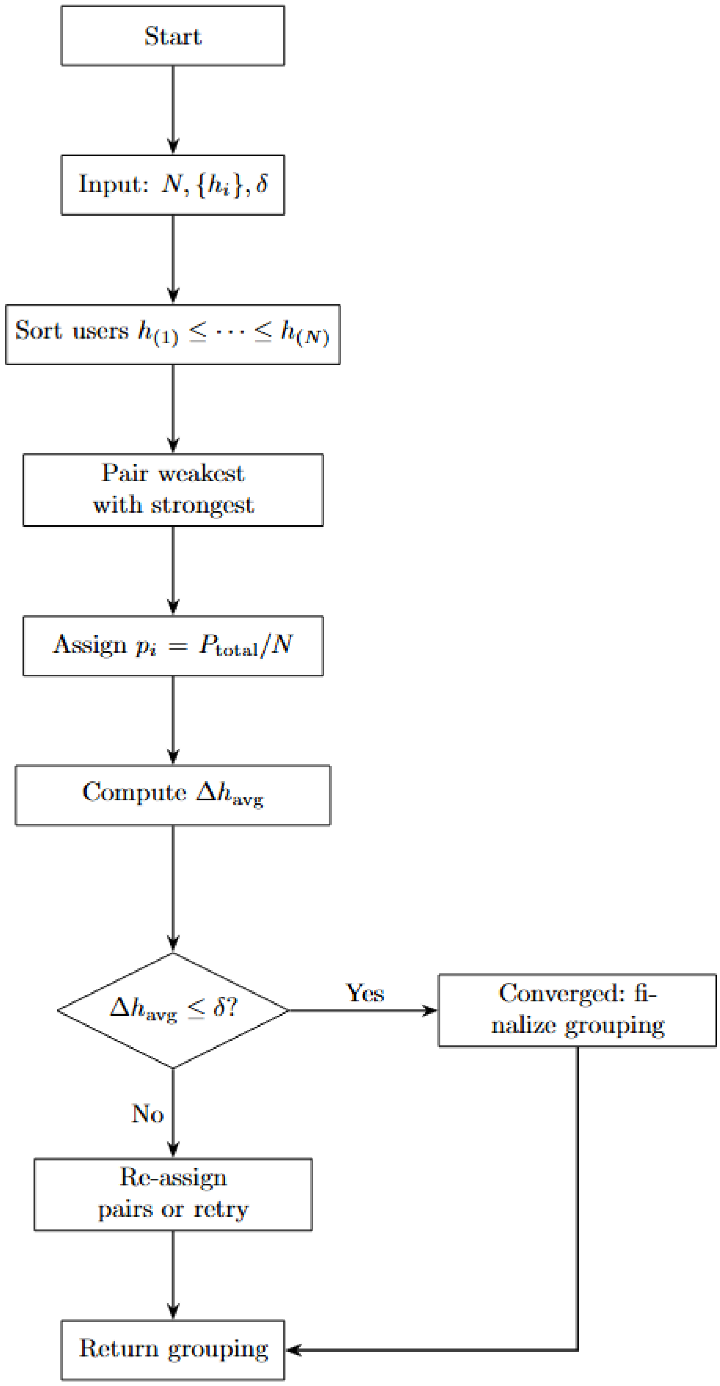

Figure 3.12: Flowchart of initialization & detection algorithm for MCGAD NOMA

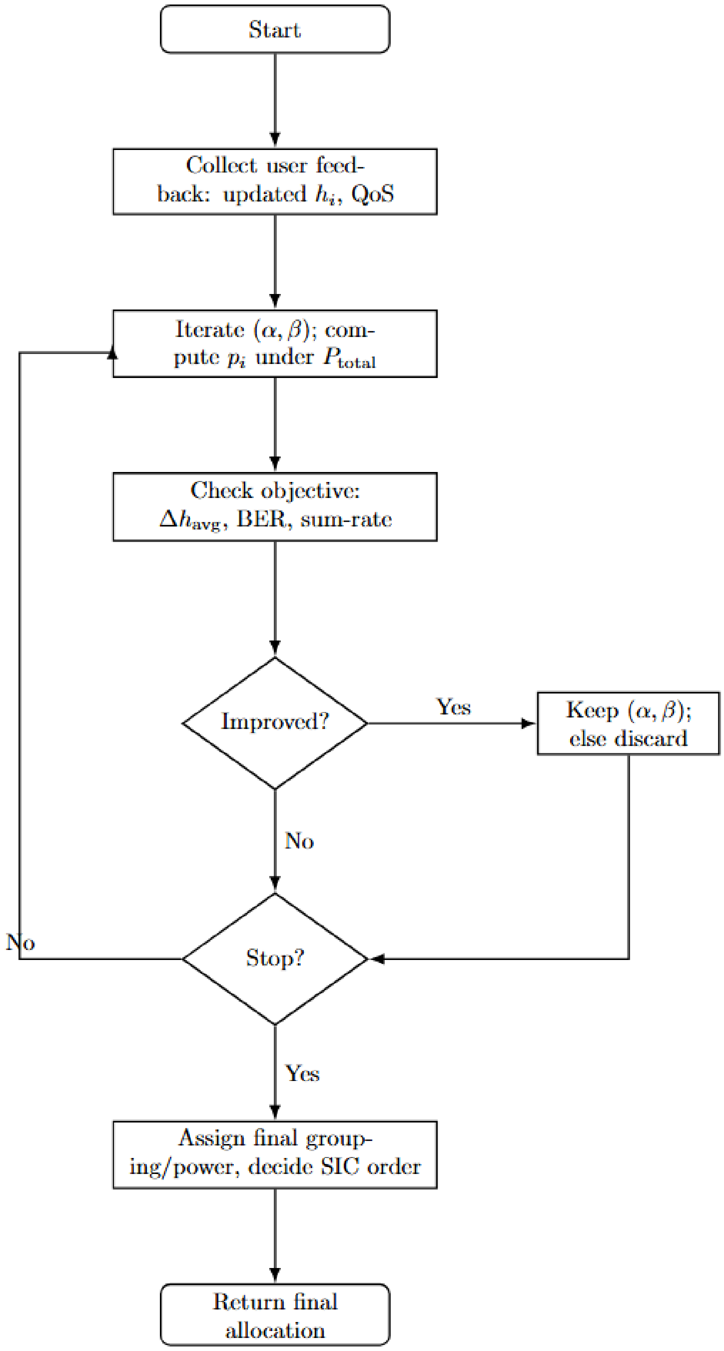

Figure 3.13: Flowchart of power allocation and four-user pairing for MCGAD NOMA

3.5 Summary

In this chapter, a comprehensive system model for indoor VLC has been established, placing particular emphasis on the synergy between ADO-OFDM and multi-user NOMA. The discussion began by examining the fundamental optical channel characteristics under a Lambertian source assumption, together with the essential signal models, performance metrics, and capacity constraints relevant to VLC links. These preliminary analyzes provided the theoretical foundation necessary for exploring advanced user multiplexing strategies in scenarios where channel conditions can vary significantly.

Subsequently, an integrated ADO-OFDM NOMA approach was introduced, illustrating how the interplay of ACO-OFDM and DCO-OFDM can enhance spectral efficiency and mitigate clipping distortion. Power-domain multiplexing and iterative SIC were then shown to accommodate both two-user and more complex multi-user scenarios, demonstrating how the proposed system adapts to diverse indoor network conditions.

To address the inherent complexities of grouping and power allocation in dense VLC environments, the MCGAD NOMA with its grouping scheme was presented. This method aims to minimize channel disparities while simultaneously refining power coefficients through iterative adjustments. The three-phase flow, encompassing initialization, optimization, and selection, ensures that user clustering remains responsive to changing conditions and effectively balances throughput, fairness, and energy efficiency.

Although multi-user decoding and iterative power allocation inevitably introduce additional computational overhead, analysis in this chapter suggests that these factors remain within practical limits for indoor VLC. The upcoming chapter will evaluate the proposed schemes under various user distributions and channel conditions, thereby highlighting the performance gains and practical viability of the integrated ADO-OFDM NOMA in real-world scenarios.

Chapter 4

Simulation Studies and Results

4.1 Introduction

The purpose of this chapter is to examine the performance of our proposed *ADO-OFDM NOMA* and *MCGAD* approaches under realistic indoor VLC conditions, focusing on key metrics such as spectral efficiency, energy efficiency, and bit error rate. In particular, we aim to illustrate how ADO-OFDM NOMA exploits both ACO-OFDM and DCO-OFDM modulation to achieve high-speed data transmission, and how a refined user-grouping algorithm based on MCGAD can further enhance multi-user resource allocation.

Figure 4.1 depicts the illustration of simulation environment, wherein we evaluate the proposed ADO-OFDM NOMA and MCGAD NOMA with their grouping schemes to handle different user distributions. The indoor environment is set to a $5\,\mathrm{m} \times 5\,\mathrm{m} \times 3\,\mathrm{m}$ room, with a single LED luminaire (Lambertian order $m = 1$) placed at the center of the ceiling. Users are distributed randomly on a horizontal plane $0.75\,\mathrm{m}$ above the floor, allowing us to capture varying channel conditions and potential interference factors. This setup reflects typical small-scale to medium-scale indoor environments such as conference rooms or exhibition halls where line-of-sight optical links remain feasible, yet user mobility and signal occlusion can reduce link quality.

Previous studies have shown that ADO-OFDM, by splitting odd and even subcarriers into ACO-OFDM and DCO-OFDM components, can mitigate clipping effects while retaining strong spectral efficiency. However, most conventional multi-user systems rely on simpler, sometimes rigid, power-

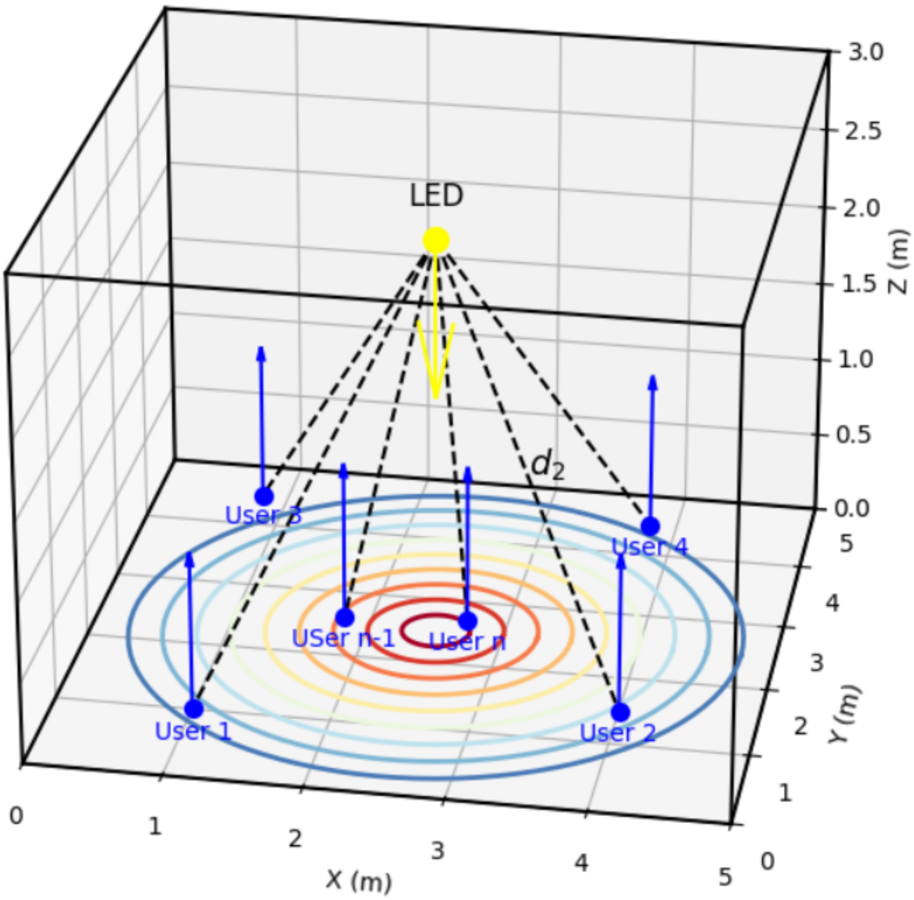

Figure 4.1: Illustration of simulation environment for ADO-OFDM NOMA and MCGAD NOMA in Multi-user VLC.

allocation or grouping methods (e.g., MCGD). In contrast, the MCGAD algorithm introduced here aims to adaptively organize users into groups that share similar average channel strengths, thereby reducing disparities and improving overall reliability. Although such grouping inherently increases computational overhead, we demonstrate in this chapter that the resulting gains in both fairness and throughput justify this added complexity for typical indoor VLC scenarios.

Up to now, there has been limited work on combining ADO-OFDM with a dynamically reconfigurable grouping strategy in VLC, particularly when user positions and channel conditions vary over time. Accordingly, the numerical simulations in this chapter are intended to highlight two main points. First, ADO-OFDM NOMA effectively capitalizes on the inherent benefits of optical OFDM to handle moderate user counts and data rate requirements. Second, MCGAD extends these benefits to denser user environments, balancing high aggregate capacity with reduced bit error rates. By evaluating multiple user densities, power-allocation ratios, and interference patterns, we offer new insights into the design of flexible, high-performance VLC systems suitable for indoor environments such as lecture halls, trade-fair pavilions, or stadiums.

The remainder of this chapter is organized as follows. We first outline the simulation parameters and relevant performance metrics. We then present the ADO-OFDM NOMA results, analyzing how its subcarrier splitting and power-domain multiplexing bolster throughput and energy efficiency. Afterward, we apply MCGAD-based grouping to larger user sets, comparing its outcomes against a baseline MCGD method to underscore the advantages of minimizing average channel disparities. Ultimately, the findings herein serve as a foundation for the comprehensive discussion of system scalability and robustness in the subsequent sections of this thesis.

4.2 Simulation Parameters and Settings

This section defines the simulation environment and parameter choices for evaluating the proposed ADO-OFDM NOMA and MCGAD algorithms under indoor VLC conditions. Emphasis is placed on reflecting practical hardware constraints, computational feasibility, and the interplay between user distribution, power allocation, and modulation efficiency.

4.2.1 Performance Metrics and Constraints

In this work, the system performance is primarily evaluated by three key performance metrics: *Bit Error Rate*, *Spectral Efficiency*, and *Energy Efficiency*. These metrics capture different yet complementary aspects of the communication link, ranging from reliability and bandwidth utilization to energy consumption.

Bit Error Rate (BER) quantifies the reliability of data transmission by measuring the fraction of received bits that are erroneously detected. It is strongly influenced by the overall signal quality, which depends on the channel conditions, modulation format, and interference level. A lower BER generally signifies more robust communication, ensuring that users can decode transmitted data with minimal errors.

The BER for ACO-OFDM is given by:

$$\mathrm{BER}_{\mathrm{ACO}} = \frac{N_{\mathrm{err,ACO}}}{N_{\mathrm{total,ACO}}} \tag{4.1}$$

For DCO-OFDM, the BER is:

$$\mathrm{BER}_{\mathrm{DCO}} = \frac{N_{\mathrm{err,DCO}}}{N_{\mathrm{total,DCO}}} \tag{4.2}$$

For ADO-OFDM, if both parts carry an equal number of bits, the BER is calculated accordingly. Otherwise, if N_{ACO} and N_{DCO} represent the total bits carried by ACO and DCO respectively, a weighted average is used:

$$\mathrm{BER}_{\mathrm{ADO}} = \frac{N_{\mathrm{ACO}}\,\mathrm{BER}_{\mathrm{ACO}} + N_{\mathrm{DCO}}\,\mathrm{BER}_{\mathrm{DCO}}}{N_{\mathrm{ACO}} + N_{\mathrm{DCO}}} \tag{4.3}$$

The bit error rate (BER) of the MCGAD system is given by:

$$\mathrm{BER}_{MCGAD} = \frac{N_{ADO1}\mathrm{BER}_{ADO1} + N_{ADO2}\mathrm{BER}_{ADO2}}{N_{ADO1} + N_{ADO2}} \tag{4.4}$$

Each ADO group's BER is computed using channel gain weighting:

$$\mathrm{BER}_{ADO1} = \frac{G_{\mathrm{ACO1}}\mathrm{BER}_1 + G_{\mathrm{DCO2}}\mathrm{BER}_2}{G_{\mathrm{ACO1}} + G_{\mathrm{DCO2}}} \tag{4.5}$$

$$\mathrm{BER}_{ADO2} = \frac{G_{\mathrm{ACO3}}\mathrm{BER}_3 + G_{\mathrm{DCO4}}\mathrm{BER}_4}{G_{\mathrm{ACO3}} + G_{\mathrm{DCO4}}} \tag{4.6}$$

where:

- N_{ADO1}, N_{ADO2} are the total bits transmitted by ADO1 and ADO2.
- G_{ACO}, G_{DCO} are the channel gains for ACO-OFDM and DCO-OFDM users.
- BER_i represents the individual BER of each user.

This formulation accounts for channel gain differences and bit distribution imbalance in the MCGAD system.

Besides these core metrics, several practical constraints also affect system design and performance. For instance, the LED must operate within its linear intensity range to avoid nonlinear distortions, environmental factors such as ambient light and user mobility can further influence channel quality. In subsequent sections, we analyze how the proposed schemes optimize BER, SE, and EE under these constraints, illustrating the trade-offs among reliability, bandwidth utilization, and energy consumption.

In a multi-user VLC network, especially one employing NOMA and ADO-OFDM, interference arises from several factors. Generally, we make an AWGN assumption to model shot noise, thermal noise, and other independent disturbances. Modeling noise as AWGN simplifies theoretical analysis and system-level simulations, making it easier to derive performance metrics such as BER, SE, and EE.

4.2.2 Total Throughput

The throughput (bits/s) of an OFDM-based system formula is:

$$T_{\mathrm{total}} = \frac{\frac{N}{2}\log_2(M)}{T_s} \tag{4.7}$$

$$T_s = \frac{N}{2B} \tag{4.8}$$

$$T_{\mathrm{total}} = \frac{\frac{N}{2}\log_2(M)}{\frac{N}{2B}} = B\log_2(M) \tag{4.9}$$

Symbol meanings:

- N: the FFT size (total number of subcarriers, of which $\frac{N}{2}$ are positive-frequency),
- B: the total system bandwidth,
- M: the modulation order in bits per subcarrier symbol,
- T_s: the OFDM symbol duration (excluding guard intervals).

This derivation shows that, in an *idealized* scenario (no error rate, no overhead), the throughput depends only on the system bandwidth B and the modulation order M.

4.2.3 Total Power Consumption

Beyond throughput, modern communication systems must also consider total power requirements to optimize energy efficiency. While the model in [41] captures distinct operational states (full load, half load, and sleep), we adapt it to visible light communication (VLC) by focusing on LED emission efficiency and fixed overhead. Specifically, the *total power consumption* P_{total} can be approximated by:

$$P_{\text{total}} = \frac{P_{\text{opt}}}{\eta_{\text{LED}}} + P_{\text{proc}} + P_{\text{circ}}, \tag{4.10}$$

where P_{opt} is the optical power required for both illumination and data transmission, η_{LED} denotes the LED efficiency (mapping optical power to electrical input), and P_{proc} and P_{circ} represent the power consumption of the digital processing and other fixed circuitry, respectively. By incorporating this simplified VLC-based model, networks can more accurately allocate power and thereby improve energy efficiency under various traffic conditions.

4.2.4 Spectral Efficiency (SE)

Spectral efficiency indicates how effectively the system utilizes its allocated bandwidth.

From (4.9) and (4.10), if B is the total system bandwidth, the SE(bits/s/Hz) is given by:

$$\mathrm{SE} \; = \; \frac{T_{\mathrm{total}}}{B} \tag{4.11}$$

This metric is particularly relevant in VLC systems, where thermal constraints and power budgets can be critical[42]. A higher SE implies transmitting more bits per unit of frequency and is essential in bandwidth-limited scenarios.

4.2.5 Energy Efficiency (EE)

Energy efficiency EE(bits/J) indicates how many bits are transmitted per unit of energy consumed:

$$\mathrm{EE} = \frac{T_{\mathrm{total}}}{P_{\mathrm{total}}} \tag{4.12}$$

A higher value of EE implies that the system can deliver more data using the same amount of energy, which is crucial in power-constrained scenarios.

4.2.6 Numerical Evaluation Parameters and Settings

Table 4.1 summarizes the main parameters and their default values employed in this thesis. The analysis focuses on: Analyzing the computational complexity and the convergence speed of the power allocation and user-grouping algorithms to assess their feasibility for real-time or near-real-time deployment in VLC networks. This involves examining how quickly and reliably the algorithms arrive at an acceptable solution, especially under dynamic channel conditions.

In the following chapters, we will illustrate how various power allocation strategies and user grouping schemes influence the these metrics, highlighting the trade-offs that emerge in practical VLC implementations.

4.2.7 Room Configuration and VLC Channel Model

We consider a $5\,\mathrm{m} \times 5\,\mathrm{m} \times 3\,\mathrm{m}$ indoor environment, representative of typical conference rooms or medium-scale office spaces. A single LED luminaire is placed at the ceiling center ($2.5\,\mathrm{m}$ above the floor), with a Lambertian order of $m = 1$ to approximate commercial white LEDs and guarantee broad

Table 4.1: Simulation Parameters and Settings

Parameter	Value
Room Size	5.0 m, 5.0 m, 3.0 m
Position of the LED	2.5 m, 2.5 m, 2.5 m
Light emission height of the LED	2.5 m
LED half-power angle ($\phi_{1/2}$)	60°
Lambertian Order (m)	1
PD field-of-view angle (ψ_{FOV})	45°
Physical area of size PD	0.5 mm × 0.5 mm
PD responsivity (R_p)	0.48 A/W
Refractive index of concentrator (n)	1.5
Optical filter gain (T_s)	1
Optical power of LED	1 W
QAM constellation size	16
Number of users (n)	4 to 20
Bandwidth	20 MHz
No. of trials	10,000

illumination coverage. The photodiode (PD) receivers are located on a plane 0.75 m above the floor, with a detection area of $0.5\,\text{mm}^2$, a field of view (FOV) of 45°, and a responsivity of 0.48 A/W. As in prior literature, an additive white Gaussian noise (AWGN) channel model is adopted for the primary line-of-sight (LOS) path, while first-order wall reflections can optionally be included to capture diffuse multipath effects.

4.2.8 ADO-OFDM NOMA for Two-user and Multi-user Scenarios

The transmitter employs an ADO-OFDM structure combining ACO-OFDM on odd subcarriers and DCO-OFDM on even subcarriers. This ensures unipolarity while enhancing spectral efficiency and mitigating clipping distortion. We further integrate NOMA in a power domain, allowing two or more users to share the same frequency resources under different power levels. For the **two-user** case, we focus on $\alpha = -7\,\text{dB}$ and $\alpha = -10\,\text{dB}$ to illustrate how a lower or higher relative power split impacts BER, SE, and EE. By comparing these two power settings, we can observe trade-offs in interference, transmission rate, and overall link quality.

4.2.9 MCGAD NOMA for Four-user and Multi-user Scenarios

When extending to four-user or denser user deployments, an adaptive grouping mechanism is essential to avoid severe performance degradation caused by inter-user interference. To this end, we compare a conventional *maximizing channel-gain difference* (MCGD) scheme to our proposed *minimizing channel-gain average difference* (MCGAD) approach. Both methods are evaluated under dynamic user positioning:

- **MCGD**: Partitions users so that high-gain and low-gain users fall into different groups but may produce imbalanced load or suboptimal fairness.
- **MCGAD**: Iteratively adjusts grouping to reduce the average gain difference within each group, potentially improving BER, fairness, and throughput.

In the MCGAD approach, users' channel gains are periodically fed back to the transmitter to update group assignments and refine power allocation via two additional parameters, α and β. Sensitivity analyses are performed over various user densities and channel conditions, measuring both computational time (for each grouping iteration) and key performance metrics such as sum rate, average BER, and energy efficiency.

Regarding user distribution and mobility, simulations allow for random placement or prescribed trajectories, such as random walks, thereby reflecting conditions encountered in typical indoor environments. During runtime, the simulator periodically measures channel gains, received signal strength, and interference patterns, enabling the evaluation of system reliability.

In terms of performance metrics, the BER serves as a foundation for comparing the different OFDM approaches under NOMA. Complementary measures include energy efficiency (quantifying how effectively power is utilized) and spectral efficiency (expressed in bits/s/Hz). The studies also investigate how capacity scales with the number of users, offering a broad view of each method's advantages or limitations.

4.3 Simulation Scenarios

In examining the proposed ADO-OFDM NOMA framework under a range of traffic and spatial conditions, we first focus on low-load scenarios (two to four active users) to highlight how the choice of the power-allocation parameter α affects individual BER and overall spectral efficiency. Conventional ACO-OFDM and DCO-OFDM schemes are used as baseline references to underscore the gains achieved by merging their best features in an ADO-OFDM structure. Specifically, we explore two-user ADO-OFDM NOMA cases at different clipping levels such as 10 dB and 6 dB to quantify the interplay among DC bias, clipping noise, and per-user power distribution.

When the user load increases beyond four, a more robust strategy is required to preserve fairness and efficiency among potentially diverse channel conditions. To address this, we introduce the MCGAD approach for multi-user grouping. Rather than simply maximizing the contrast in channel gains (as in some conventional user-grouping schemes), MCGAD strives to reduce large disparities within each group. This design not only mitigates severe interference in the power domain but also helps balance resource allocation across multiple users. In high-load conditions, the synergy between ADO-OFDM's spectrally efficient modulation and MCGAD's adaptive grouping becomes particularly valuable: it manages both local imbalances (by tuning α for each user set) and global fairness (by separating users into cohesive groups).

Although the physical layout of LED transmitters can play a pivotal role in real deployments, the results in this chapter focus primarily on single-LED scenarios. Positioning a single luminaire in the center of the room simplifies coverage analysis and allows a direct assessment of how MCGAD and ADO-OFDM NOMA respond to corner users or partial occlusions. In more complex configurations e.g., multiple LEDs distributed to cover a large hall these techniques can be extended to coordinate power allocation among overlapping cells, provided that the feedback and grouping mechanisms remain scalable.

Under all scenarios, the overarching theme is to balance energy usage and bandwidth utilization. By maintaining a finite power budget, we investigate how aggressively power-saving strategies can be applied before spectral efficiency deteriorates. The simulation results presented in the following section compare different clipping levels, user positions, and group sizes to reveal the relative benefits of ADO-OFDM NOMA under both light and heavy user loads. Moreover, we demonstrate how MCGAD refines resource distribution when multiple users compete for limited optical power, ultimately preserving lower BER and higher aggregate throughput than simpler grouping methods.

4.4 Simulation Results

4.4.1 Evaluation Performance of ADO-OFDM NOMA

In this subsection, we focus on the performance of a two-user ADO-OFDM NOMA system under different DC bias levels and user-location scenarios. We begin by examining the BER performance at a transmit signal-to-noise ratio (SNR) of $E_{\mathrm{b,opt}}/N_0 = 125\,\mathrm{dB}$, with DC bias values of $10\,\mathrm{dB}$ and $6\,\mathrm{dB}$. Figures 4.2 and 4.3 illustrate how the BER of both users, denoted as user 1 and user 2, evolves as the power allocation factor α varies.

As shown in Fig. 4.2, when the DC bias is set to $10\,\mathrm{dB}$ and the two users are located relatively close to each other, a smaller α allocates more transmit power to user 1, thus reducing its BER. However, as user 2 consequently receives less power, its BER increases. When α becomes larger, the performance of user 2 improves at the cost of heightened clipping noise for user 1, which may be amplified during successive interference cancellation (SIC), eventually degrading user 1's detection accuracy.

Meanwhile, in Fig. 4.3, both users are located farther apart, and the DC bias is lowered to $6\,\mathrm{dB}$. Under these conditions, it is often necessary to shift the optimal α toward more negative values (e.g., from $-5\,\mathrm{dB}$ to around $-11\,\mathrm{dB}$) to compensate for the weaker channel gain of the distant user. Furthermore, reducing the DC bias increases clipping noise, forcing the system to allocate more power to the DCO-OFDM component to keep the BER within acceptable ranges.

In addition to the BER analysis, we provide two more figures (Figs. 4.4

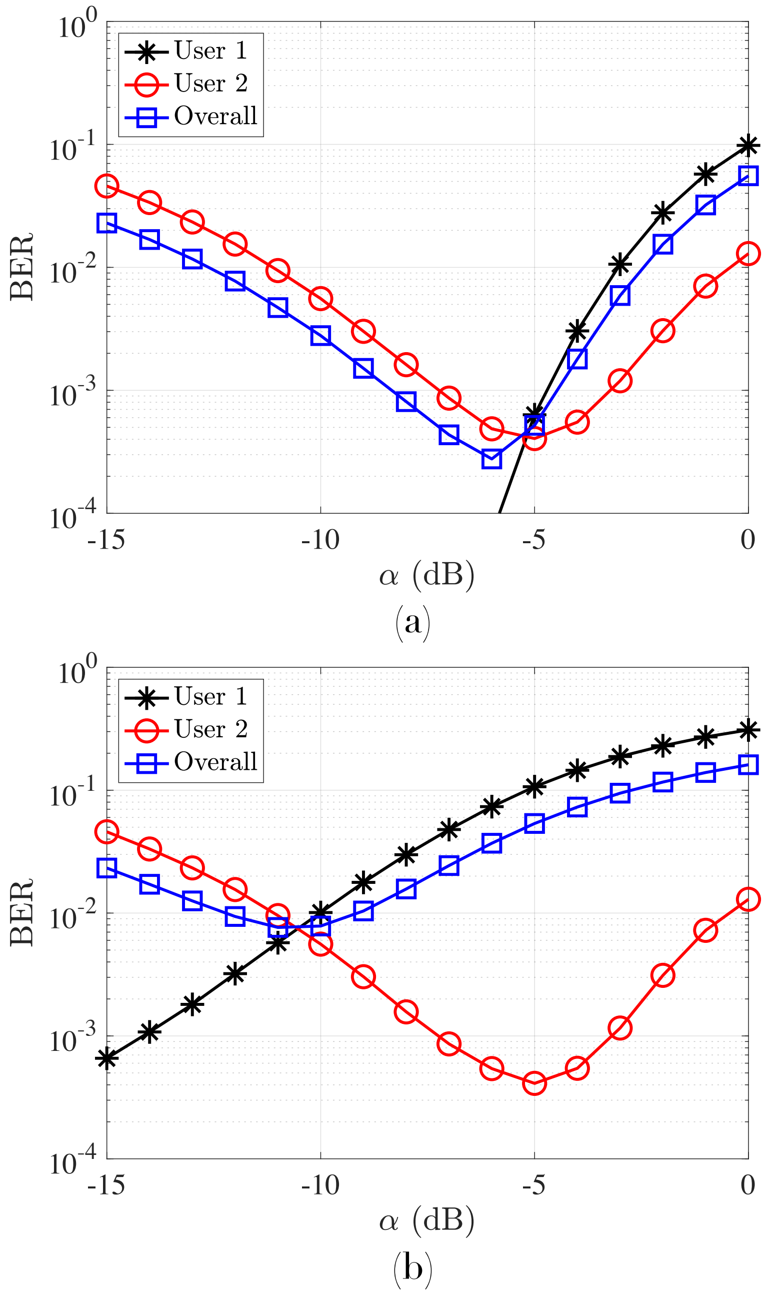

Figure 4.2: BER vs. α when two users are closely spaced with a 10 dB DC bias.

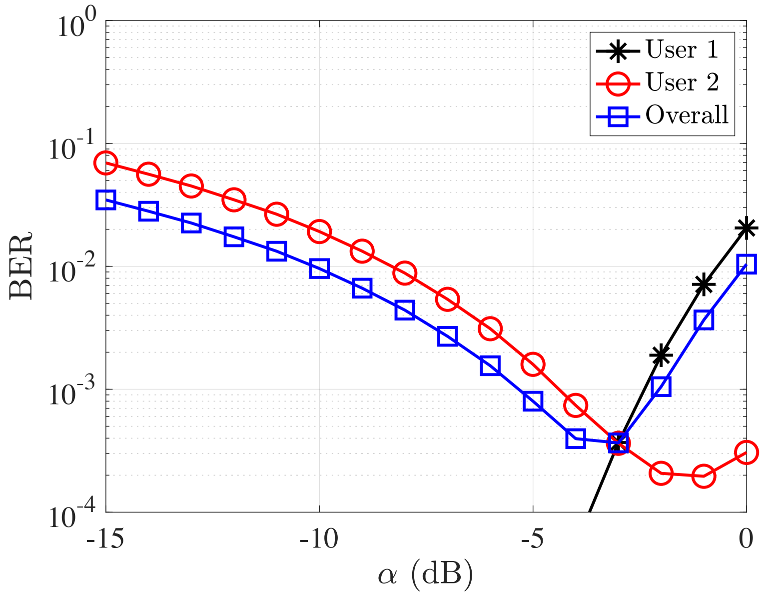

(a)

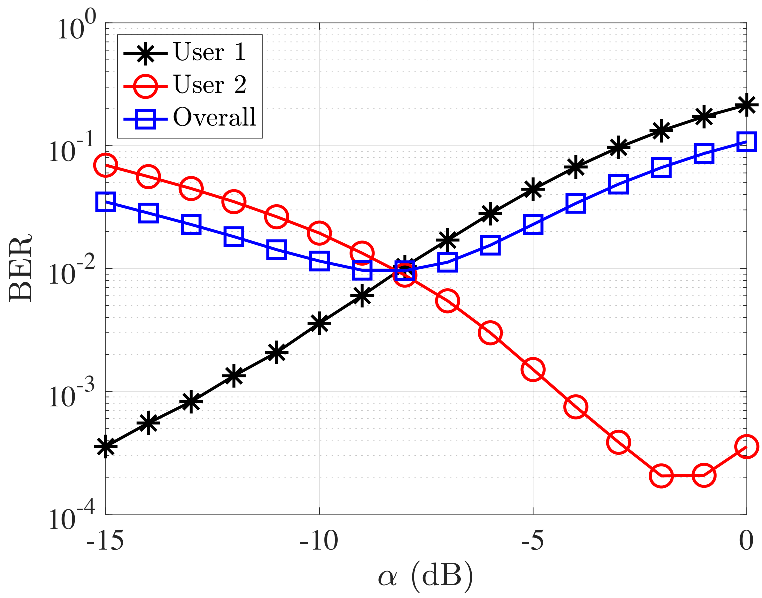

(b)

Figure 4.3: BER vs. α when two users are farther apart with a 6 dB DC bias.

and 4.5) to demonstrate how ADO-OFDM NOMA compares to other OFDM-based schemes in terms of energy efficiency and spectral efficiency, under varying numbers of users. These results further highlight the advantages and trade-offs of ADO-OFDM NOMA in multi-user scenarios.

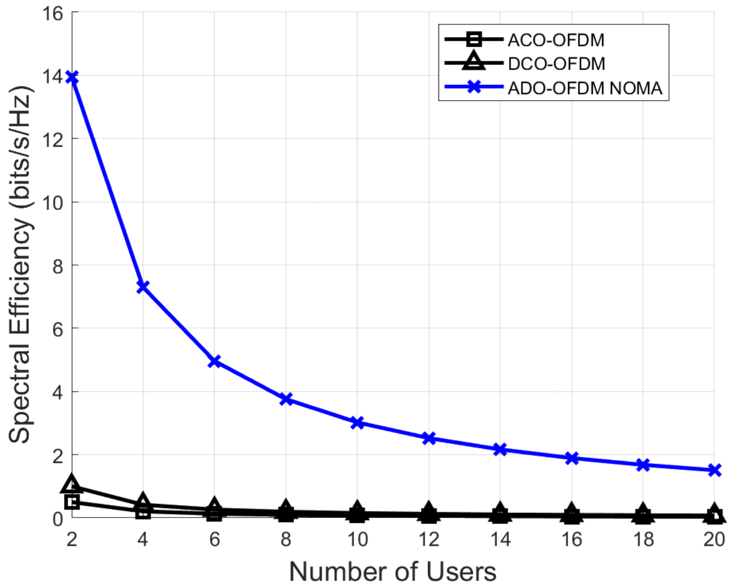

Figure 4.4: Performance of spectral efficiency versus no. of users

As illustrated in Fig. 4.13, ADO-OFDM NOMA can maintain higher energy efficiency (in bits/J) compared to traditional approaches, owing to the flexible power allocation strategy that can adapt to varying channel conditions. Nevertheless, with an increasing number of users, the system inevitably faces stronger inter-user interference and increased clipping noise, resulting in some efficiency degradation. Figure 4.14 shows that ADO-OFDM NOMA also offers benefits in terms of spectral efficiency, as it enables simultaneous transmission to multiple users on overlapping frequency resources. However, balancing the spectral efficiency and the BER performance of individual users remains critical—if α is not properly chosen, one user's link quality may suffer significantly at the expense of another.

As shown in Figure 4.6, the parameter α in an ADO-OFDM system (often indicating the proportion of power allocated to the ACO-OFDM part) decreases as the number of users N increases. When $N = 2$, $\alpha \approx 0.6$, while

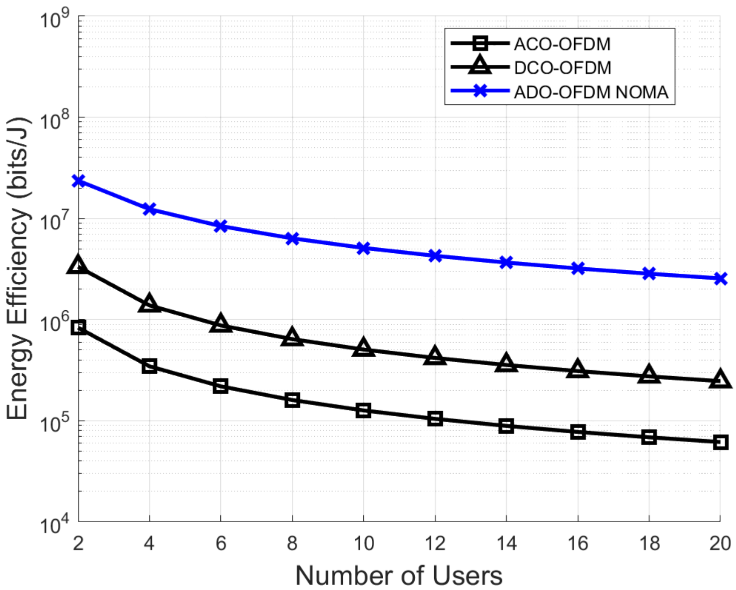

Figure 4.5: Performance of energy efficiency versus no. of users

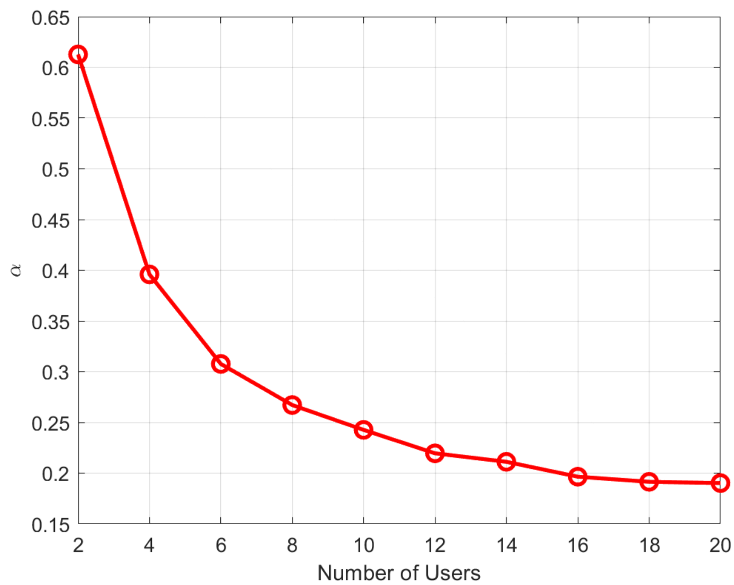

Figure 4.6: Performance of α versus no. of users for ADO-OFDM NOMA

at $N = 20$, α has dropped to around 0.17. This monotonic decrease is primarily because as more users join the system, the power allocated to each user becomes smaller. To meet the overall optical power and modulation constraints, the portion of power dedicated to ACO-OFDM must be reduced, leading to a continued decline in α as N grows.

4.4.1.1 Average α and β versus Number of Users

Next, we investigate how the power-ratio parameters α and β evolve as the number of users increases. Figures 4.7 and 4.8 show the average values of α and β, respectively, after convergence of the MCGAD grouping and iterative power allocation. When the network size is small, α tends to be larger to ensure that each group receives sufficient power, thereby preserving service quality for all users. However, as more users join, the algorithm systematically reduces α while fine-tuning β to maintain fairness across multiple groups. This behavior reflects a similar trend observed in the two-user case (cf. Section 4.4, Figs. 4.2 and 4.3), where an imbalanced choice of α could quickly degrade one user's BER.

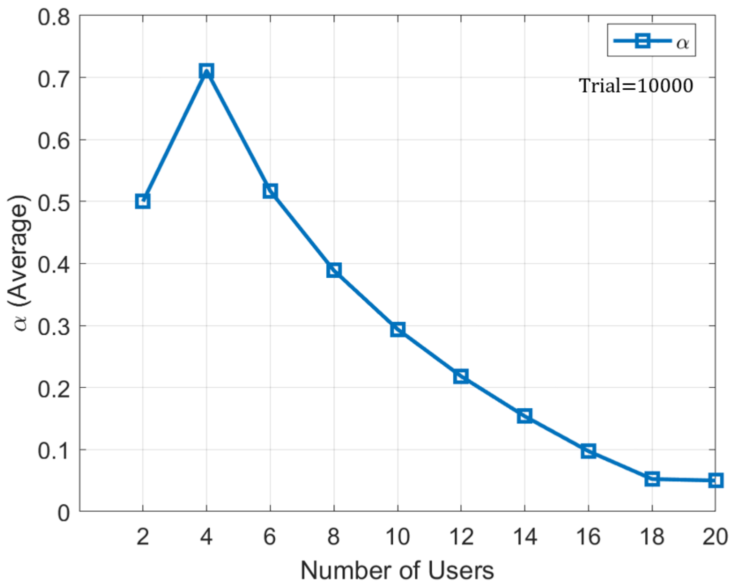

Figure 4.7: Performance of average α versus no. of users for MCGAD NOMA

4.4.1.2 BER for Extended Scenarios

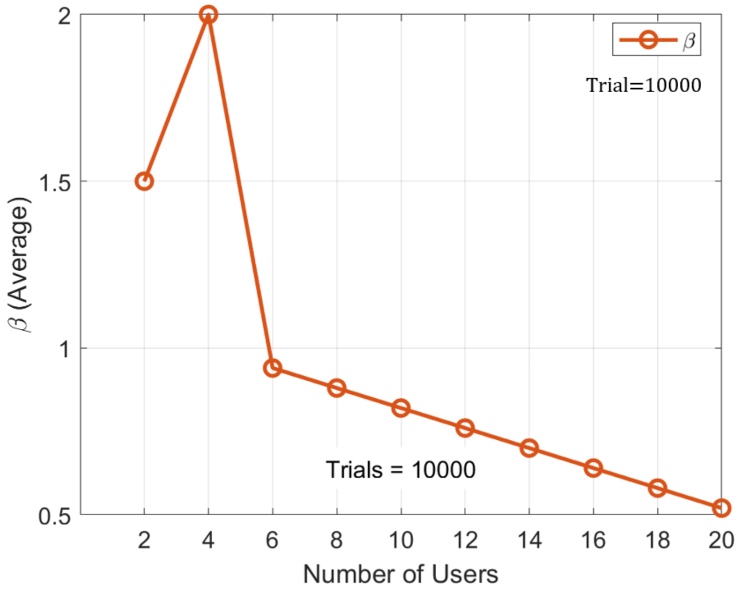

Figure 4.8: Performance of average β versus no. of users for MCGAD NOMA

To further examine MCGAD's effectiveness and imbalanced LED–user distances, we present BER curves in Figure 4.9 illustrates the BER under high-SNR conditions for three schemes: MCGAD (red), ADO-OFDM NOMA (black), and MCGD (blue). Across the range of α from $-30\,\mathrm{dB}$ to $0\,\mathrm{dB}$, the BER axis is plotted on a logarithmic scale. One immediately sees that ADO_NOMA's curve remains near 10^{-1} throughout, from about 1×10^{-1} at $\alpha = -30\,\mathrm{dB}$ to a slightly lower 7×10^{-2} around $\alpha = -5\,\mathrm{dB}$, then back to 1×10^{-1} by $\alpha = 0\,\mathrm{dB}$. This comparatively flat and high BER profile suggests that under these channel conditions, standard ADO-OFDM NOMA struggles to help the weaker user.

By contrast, MCGAD steadily reduces its BER as α increases. At the leftmost point of $\alpha = -30\,\mathrm{dB}$, it achieves a BER around 3×10^{-3}, already better than ADO-OFDM NOMA. It then declines further toward a distinct minimum near $\alpha = -8\,\mathrm{dB}$, where the curve dips close to 2×10^{-5}. Although it starts to rise again if α passes $-5\,\mathrm{dB}$, MCGAD's BER at $\alpha = 0\,\mathrm{dB}$ is still on the order of 10^{-3}—an improvement of nearly two orders of magnitude compared to ADO-OFDM NOMA's persistent 10^{-1} region. Meanwhile, MCGD shows an even more pronounced improvement around $-10\,\mathrm{dB}$ to

$-8\,\text{dB}$, reaching an exceptionally low BER of about 1×10^{-6}. This outcome highlights the scheme's ability to allocate power effectively when pairing extremely weak and strong users, but it also exhibits more sensitivity to shifts in α. Performance climbs sharply above 10^{-4} once α exceeds $-5\,\text{dB}$, and at the left edge near $-30\,\text{dB}$, the BER remains around 10^{-2}, which, while still superior to ADO-OFDM NOMA, lags behind MCGAD NOMA.

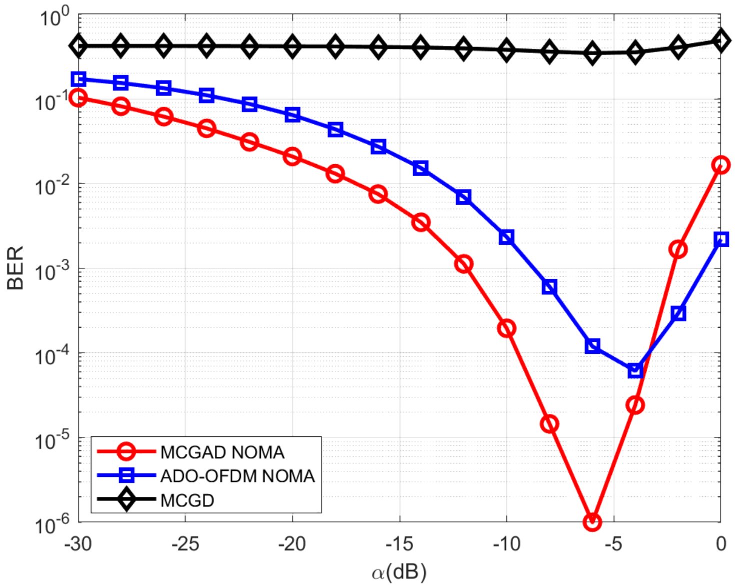

Figure 4.9: Performance of BER versus α for various schemes in four-user VLC scenario

Overall, Figures 4.2 and 4.3 confirm the importance of carefully tuning α and the DC bias to meet user-specific BER requirements, whereas Figures 4.4 and 4.5 provide additional insight into the system's energy and spectral efficiency behaviors. These outcomes collectively demonstrate that while ADO-OFDM NOMA enhances multiuser performance through flexible power allocation, it also introduces new challenges in terms of managing inter-user interference, clipping noise, and user fairness—factors that must be jointly considered in system design.

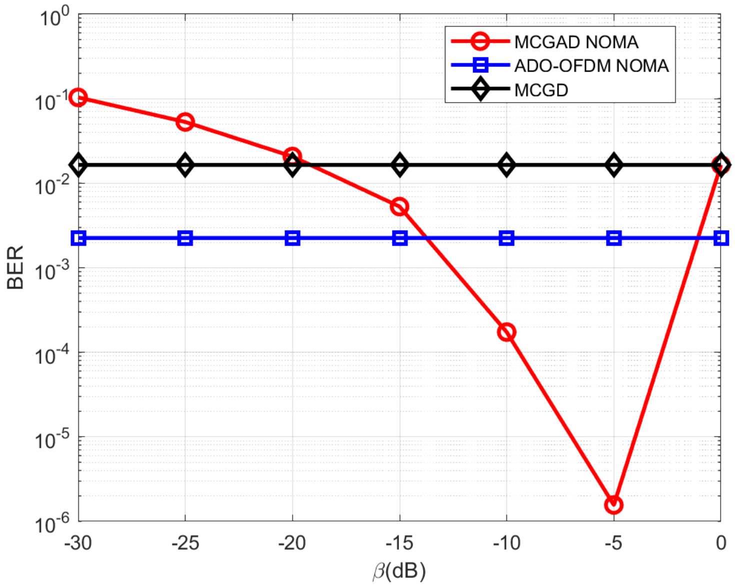

Figure 4.10: Performance of BER versus β for various schemes in four-user VLC scenario

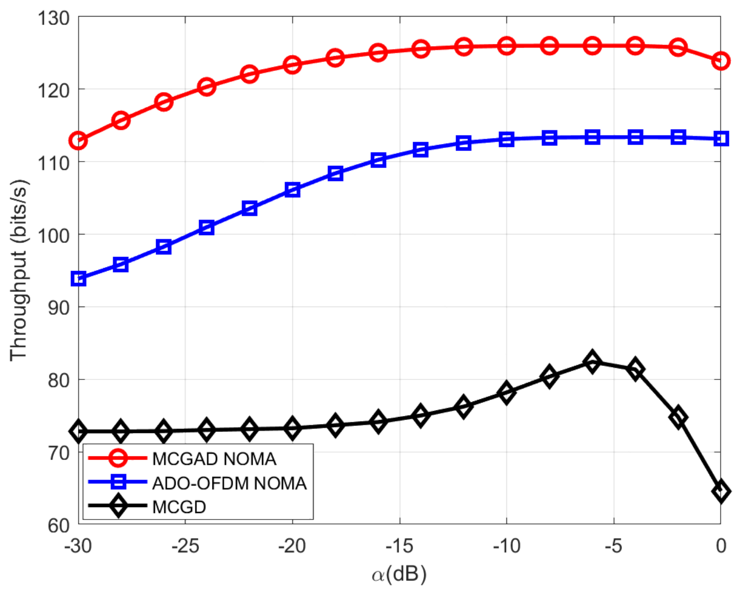

Figure 4.11: Performance of throughput versus α for various schemes in four-user VLC scenario

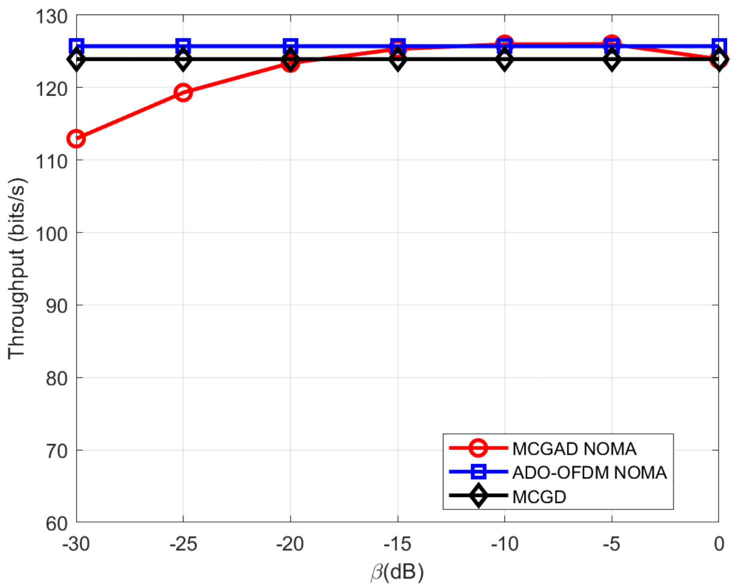

Figure 4.12: Performance of throughput versus β for various schemes in four-user scenario

4.4.2 Multi-user NOMA Performance with MCGAD Grouping

As the number of users grows beyond four, the performance benefits of ADO-OFDM NOMA become more dependent on effective grouping and power allocation strategies. In this work, we apply our proposed MCGAD (Minimized Channel-Gain Disparity) algorithm, which clusters users with similar channel conditions into groups and then iteratively adjusts α (for ADO-OFDM NOMA) and β (for group-level power) to prevent any single user from dominating or starving in the power domain. This strategy mitigates inter-user interference and helps maintain balanced performance as the network scales.

Four-user Scenario Spectral and Energy Efficiency (Figs. 4.10 and 4.11).

In the initial evaluation stage, we consider a four-user scenario to illustrate how grouping can improve both spectral and energy efficiency (SE and EE). As shown in Fig. 4.13 (spectral efficiency) and Fig. 4.14 (energy efficiency), the proposed MCGAD scheme consistently outperforms both conventional ADO-OFDM NOMA (without grouping) and a baseline maximizing-channel-gain-difference (MCGD) algorithm. By placing users with comparable channel gains in the same group, MCGAD avoids the extreme power offsets that would otherwise be needed for users with significantly weaker links. Consequently, it makes better use of the available transmit power, leading to higher throughput (measured in bits/s/Hz) and a more favorable bits-per-joule ratio.

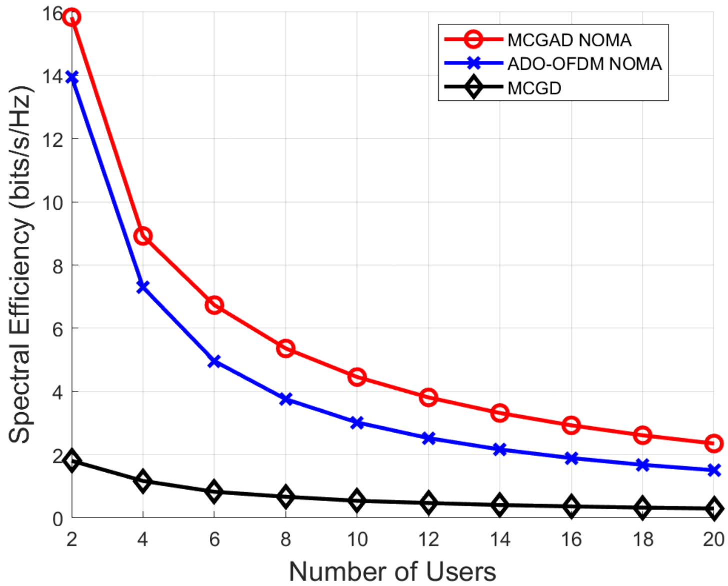

Figure 4.13: Performance of spectral efficiency for multi-user VLC scenario

Figure 4.11 provides the corresponding throughput curves. ADO-OFDM NOMA, starting at about 65 bits/s when $\alpha = -30$ dB, peaks near 85 bits/s around -10 dB, then drops to 60 bits/s at $\alpha = 0$ dB. MCGAD begins at approximately 85 bits/s and gradually climbs above 110 bits/s between -15 dB and -5 dB, reflecting the region where its BER also reaches 10^{-5}. Even by $\alpha = 0$ dB, MCGAD stays above 100 bits/s, demonstrating stable performance across a wider operating range than ADO_NOMA. MCGD, for its part, achieves around 110 bits/s at $\alpha = -30$ dB and soars to nearly 130 bits/s as α approaches -10 dB. It remains above 120 bits/s in the vicinity of its best BER but declines back to around 115 bits/s by $\alpha = 0$ dB.

Overall, the plots confirm that MCGD can attain the highest peak throughput (about 130 bits/s) and the lowest BER (near 10^{-6}) in a narrow α win-

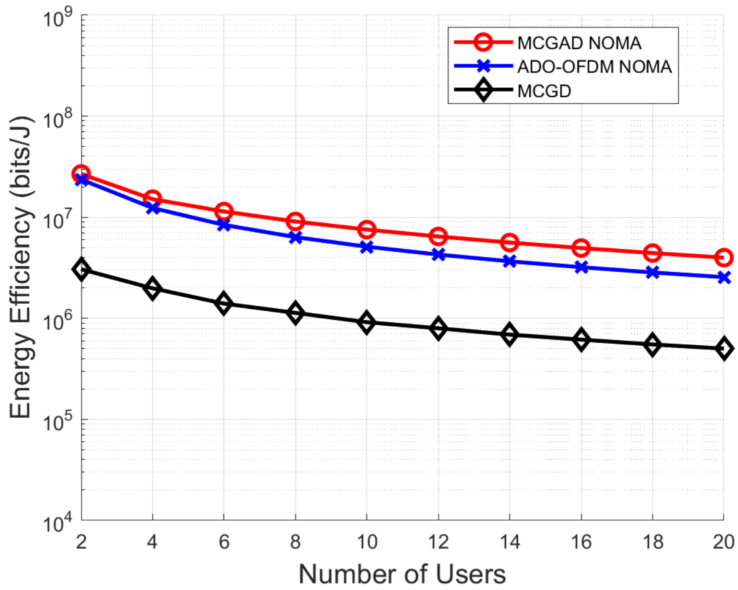

Figure 4.14: Performance of energy efficiency for multi-user VLC scenario

dow, whereas MCGAD delivers a more robust balance over a broader range, dropping to only about 10^{-5} at its best BER and maintaining well above 100 bits/s in throughput. ADO_NOMA lags both competitors here, suggesting that in these highly imbalanced LED-user scenarios, its fixed power-split strategy does not adequately compensate for the weaker user's channel losses. Nonetheless, refining decode ordering and allocating additional targeted power to the user in need could further improve ADO_NOMA or MCGD performance in setups that are not quite so extreme.

4.4.1.3 Highly User Density in a $10m \times 10m \times 3m$ Room Environment

Finally, to validate MCGAD NOMA performance in a larger spatial environment, we consider a $10m \times 10m \times 3m$ room layout. Figures 4.15 and 4.16 display 3D heatmaps for spectral and energy efficiency, respectively, as functions of α and β. These plots reveal a well-defined "sweet spot" region in which the combined allocation of α (within the ADO-OFDM NOMA) and β (applied at the group level) maximizes both SE and EE. Points outside this region result in either insufficient power to certain groups causing higher BER and lower throughput or excessive clipping noise that hurts overall performance. Hence, the proposed MCGAD NOMA systematically converges to operating points that lie near these optima, even when the network features large spatial dimensions and many simultaneously active users.

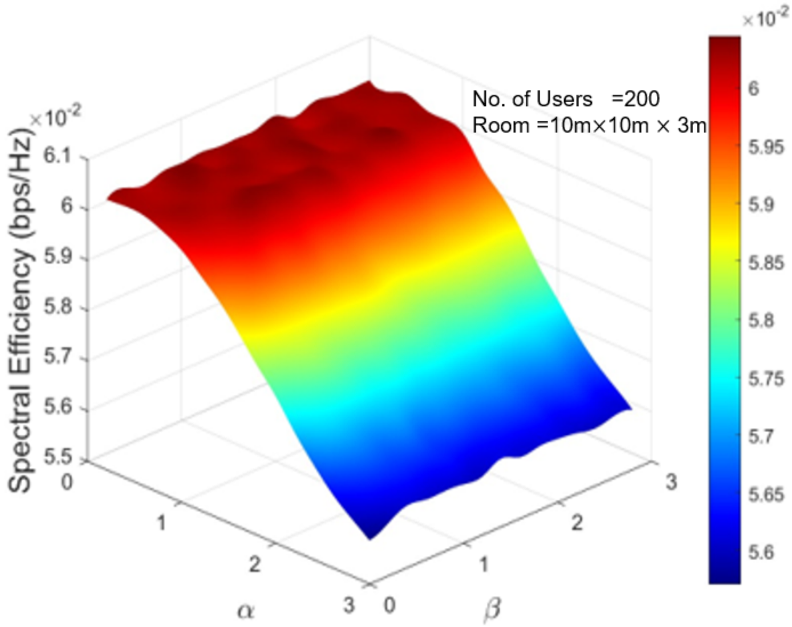

Figure 4.15: Spectral efficiency analysis in multi-user VLC

Overall, these results confirm that adaptive grouping and iterative power allocation, as implemented in the MCGAD scheme, can effectively manage multi-user scenarios with diverse channel conditions. The gains in both spectral and energy efficiency (Figs. 4.4–4.11) remain robust even under large-scale spatial deployments (Figs. 4.15–4.16). Hence, MCGAD-NOMA emerges as a promising approach for practical indoor VLC networks, where user density is high and channel heterogeneity is inevitable. Future work will refine the proposed algorithm by integrating more sophisticated decode ordering, dynamic resource allocation, and interference cancellation techniques, further broadening the viability of multi-user ADO-OFDM NOMA in next-generation VLC systems.

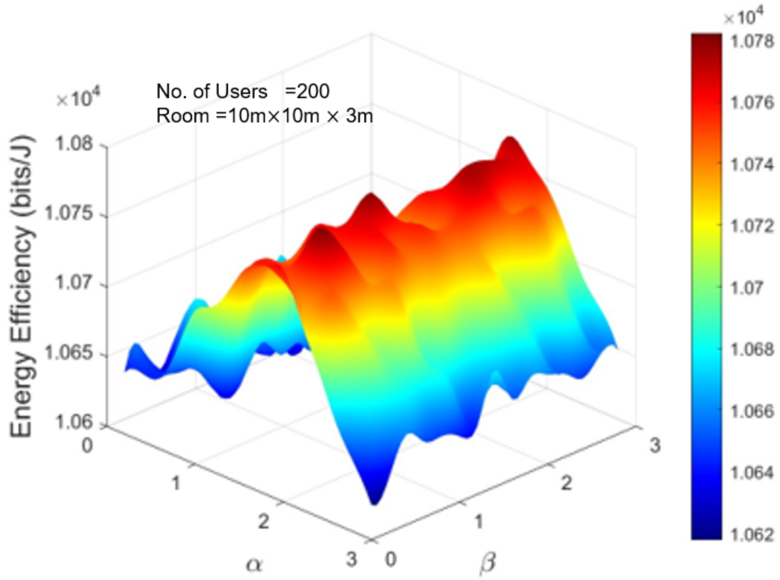

Figure 4.16: Energy efficiency analysis in multi-user VLC

Table 4.2: Summary of Evaluation Performance for ADO-OFDN NOMA

No. of Users	α	β	**BER**	**Throughput**	**SE**	**EE**
2	0.61	-	10^{-4}	112 bits/s	14 bits/s/Hz	10^6 bits/J
4	0.61	-	10^{-3}	110 bits/s	7.5 bits/s/Hz	10^7 bits/J
20	0.61	-	10^{-2}	90 bits/s	1.8 bits/s/Hz	10^5 bits/J
200	0.61	-	10^{-1}	50 bits/s	$5 * 10^{-2}$ bits/s/Hz	10^1 bits/J

4.4.3 Discussions and Implications

The results in Figures 4.4–4.11 underscore the advantages of combining ADO-OFDM NOMA with an adaptive grouping mechanism such as MCGAD. At lower user counts, Figures 4.4 and 4.6 show that even a basic ADO-OFDM NOMA configuration outperforms standalone ACO-OFDM and DCO-OFDM by leveraging both subcarrier allocations. However, as the number of users increases, those same figures reveal that MCGAD NOMA maintains noticeably higher spectral efficiency and superior energy efficiency compared to the conventional MCGD strategy or a basic ADO-OFDM NOMA without grouping.

This improved scalability primarily arises from MCGAD's ability to dis-

Table 4.3: Summary of Evaluation Performance for MCGAD NOMA

No. of Users	α	β	**BER**	**Throughput**	**SE**	**EE**
2	0.7	1.5	10^{-4}	112 bits/s	14 bits/s/Hz	10^{6} bits/J
4	0.7	1.5	10^{-5}	125 bits/s	16 bits/s/Hz	10^{7} bits/J
20	0.7	1.5	10^{-3}	80 bits/s	2 bits/s/Hz	10^{5} bits/J
200	0.9	1.2	10^{-1}	40 bits/s	$6.2 * 10^{-2}$ bits/s/Hz	10^{1} bits/J

tribute power more evenly across multiple groups, thus avoiding severe interference in the power domain. Rather than over-allocating resources to weaker or distant users—which can clip the ADO-OFDM signal—MCGAD iteratively refines group boundaries and adjusts α and β. Figures 4.8 and 4.9 illustrate how these parameters evolve as more users join the network: α initially increases to boost weaker links, then decreases once a stable grouping is established and fairness is achieved. Meanwhile, β adapts in tandem to accommodate subtle channel variations and growing multi-user interactions.

The 3D surface plots in Figures 4.10 and 4.11 further highlight the trade-offs between spectral efficiency and energy efficiency under different α–β combinations. In moderate-load scenarios, a wide range of parameter settings yields near-optimal outcomes, but as user density intensifies, finding the correct α–β region becomes crucial. These observations align with the earlier two-user analysis: although tuning α alone can mitigate moderate interference, the higher user loads demand a more holistic allocation approach. MCGAD meets this need by maintaining moderate transmit power levels while minimizing channel-gain disparities within each group.

Overall, these findings confirm that while ADO-OFDM NOMA significantly increases throughput over standalone OFDM at smaller scales, an adaptive algorithm is essential to sustain efficiency at higher user densities. Through iterative grouping and power tuning, MCGAD mitigates severe imbalances, ensures more consistent BER across all users, and retains favorable energy efficiency. Although these iterative updates add complexity, the simulation results show that the net benefits—enhanced network capacity, reduced interference, and improved fairness—outweigh the overhead in practical indoor VLC scenarios. The next chapter examines computational costs and potential optimizations to keep MCGAD viable under real-time constraints.

4.5 Summary

In this chapter, we presented a comprehensive set of simulation studies that examine the performance of ADO-OFDM NOMA in both two-user and multi-user VLC environments, along with an in-depth exploration of the proposed MCGAD NOMA grouping strategy. Beginning with a discussion of the basic system configuration, key optical parameters, and power-allocation options, we established how ADO-OFDM can effectively merge ACO-OFDM and DCO-OFDM subcarriers to balance clipping noise, spectral efficiency, and BER performance.

Under low-load scenarios, such as the two-user case, tuning the α parameter proved sufficient to improve the weaker user's link quality without excessively degrading the stronger user's performance. This highlights ADO-OFDM NOMA's flexibility in allocating power among users with differing channel conditions. However, as the user count rose above four, multi-user interference and fairness considerations necessitated more sophisticated resource allocation algorithms. By integrating our MCGAD NOMA approach, groups of users were formed in a way that minimizes large disparities in channel gains, leading to consistent improvements in both spectral and energy efficiencies compared to simpler methods.

Our results showed that MCGAD NOMA yields higher throughput, better fairness, and more stable BER across diverse channel environments, outperforming a conventional MCGD baseline. Additionally, the adaptive parameters α and β played a pivotal role in mitigating excessive clipping and balancing resource usage, making MCGAD NOMA particularly effective under heavier user loads. While the iterative nature of MCGAD introduces overhead in computation and feedback, the net gains suggest that this trade-off is viable for practical indoor VLC systems, especially when designing next-generation infrastructures such as conference halls and stadium-like venues.

Overall, the findings in this chapter confirm the potential of merging ADO-OFDM's efficient modulation with advanced NOMA scheduling to sustain high throughput, low BER, and favorable energy efficiency. This work establishes a strong foundation for further optimizations at the system level, including reducing computational complexity and extending coverage to multi-LED deployments. In doing so, it provides a pathway toward robust, scalable VLC networks where users with widely varying channel conditions can be reliably served.

Chapter 5

Conclusion

5.1 Concluding Remarks

This thesis presents a comprehensive study on enhancing multi-user VLC systems by drawing on both ACO-OFDM and DCO-OFDM technologies. VLC inherently provides wide unlicensed bandwidth, high data rates, and robust link security, yet practical challenges arise from LED nonlinearity and user mobility. As user counts increase, NOMA emerges as a critical approach for efficiently allocating spectral resources to users under varying channel conditions, thereby overcoming bandwidth constraints. By considering both ACO-OFDM's clipping-based design and DCO-OFDM's biasing strategy, a pathway is laid for flexible optical modulation that can serve users with diverse signal-to-noise ratios.

Building on these complementary techniques, this thesis introduces an integrated ADO-OFDM framework, pairing ACO and DCO schemes for efficient power and resource allocation. A dedicated *Minimizing Channel-Gain Average Difference* (MCGAD) algorithm is further proposed to handle user grouping, ensuring fair power distribution and interference management. Extensive simulations confirm that the ADO-OFDM NOMA system, enhanced with MCGAD, delivers notable improvements in throughput, spectral efficiency, and energy efficiency across various indoor deployment scenarios, including both single-LED and multi-LED coverage areas. These findings underscore the feasibility of combining ACO-OFDM, DCO-OFDM, and NOMA—augmented by adaptive grouping—for next-generation VLC networks that demand high capacity, equitable resource sharing, and energy-conscious operations.

5.2 Contributions

This thesis makes four main contributions to the research on VLC and NOMA. First, it introduces an integrated ADO-OFDM NOMA framework that merges the clipping control of ACO-OFDM and the biasing strategy of DCO-OFDM with power-domain multiplexing. This unified design allows several users to share the same frequency band, boosting resource usage while keeping clipping noise in check.

Second, a dynamic grouping algorithm called MCGAD is proposed to handle multi-user interference and power fairness in dense networks. Instead of maximizing the difference in channel gains, MCGAD places users into groups based on their channel quality and then tunes each group's power level so that no user is consistently at a disadvantage. This approach is especially helpful in crowded indoor environments where user mobility or variations in channel gain could hurt overall performance.

Third, the thesis conducts a realistic assessment of the new system under an indoor Lambertian VLC channel model, combined with AWGN. Results show that the ADO-OFDM NOMA scheme, supplemented by MCGAD, can maintain a low BER and high spectral efficiency in both single-LED settings. This flexibility highlights the system's adaptability to a range of indoor layouts.

Finally, the integrated solution enhances energy efficiency by making use of ACO-OFDM's ability to reduce energy overhead through clipping-based modulation, while assigning power intelligently among users via MCGAD. The bit-per-joule metric improves compared to traditional orthogonal approaches, which is especially valuable for large-scale IoT scenarios or cases where power consumption is a key concern.

These combined elements establish a clear and effective pathway toward efficient, adaptive, and high-capacity multi-user VLC networks, making the proposed framework a promising option for next-generation indoor wireless communication.

5.3 Future Works

Although this thesis confirms the viability of ADO-OFDM NOMA for multi-user VLC, several further research directions remain open. One is to examine larger indoor spaces featuring multiple LEDs with overlapping coverage and mixed line-of-sight (LOS) and non-line-of-sight (NLOS) channels, where more complex spatial configurations and higher interference may arise. Investigating how user grouping and power allocation adapt to these conditions would provide stronger evidence of the system's scalability, especially under significant user movement or variations in channel gain.

Another promising avenue involves applying modern machine learning methods—such as reinforcement learning, deep neural networks, or online clustering—to extend the MCGAD algorithm. By drawing on real-time data about user locations, channel variations, and mobility patterns, these techniques could dynamically optimize power distribution and user assignments, automatically reconfiguring resource usage to preserve throughput and fairness. They might also respond more effectively to unexpected environmental factors like partial occlusions, swiftly readjusting power levels, or subcarrier allocations when users move across different signal-strength regions.

From a practical standpoint, building a hardware prototype would verify how LED drivers, photodiodes, and digital signal processors interact with MCGAD-based resource scheduling. Such testing could reveal front-end nonlinearities or additional constraints that are not fully captured in theoretical models, guiding more precise hardware designs or calibration methods. In addition, security and quality-of-service (QoS) remain central for real-world adoption. While VLC's physical layer properties offer some inherent protection against eavesdropping, emerging threats may demand extra safeguards. Future work could investigate QoS-focused power allocation, dynamic beam steering, or hybrid deployments combining VLC and radio-frequency systems to ensure resilience across a variety of indoor environments.

By pursuing these directions, researchers can extend the foundations set here, helping ADO-OFDM NOMA reach its full potential in large-scale, adaptive, and energy-efficient VLC networks that meet the evolving demands of next-generation communications.

Bibliography

[1] NASA. Nasa website: Visible light spectrum. `https://www.nasa.gov/directorates/somd/space-communications-navigation-program/radio-vs-optical-spectrum/`, 2023. Accessed: 27 Sep. 2023.

[2] Cuiwei He and Chen Chen. A Review of Advanced Transceiver Technologies in Visible Light Communications. *Photonics*, 10(648):6, 2023.

[3] Mohamed I. Gabr. Data transmission via visible light communication (vlc) technique. *International Journal of Innovative Research in Science, Engineering and Technology*, 5:16473–16481, 09 2016.

[4] J. Armstrong. OFDM for optical communications. *J. Lightwave Technol.*, 27(3):189–204, 2009.

[5] H. S. O. K. and A. K. Sah. Multi-user grouping for NOMA enabled VLC system. *IEEE Commun. Lett.*, 28(5):1072–1076, May 2024.

[6] Y. Wu, X. Li, L. Sun, and X. Lin. An energy efficient power allocation method for NOMA-based VLC systems. In *Proc. Int. Conf. Intelligent Computing and Wireless Optical Communications (ICICWOC)*, pages 102–106, 2024.

[7] S. Wei and J. Ma. Resource allocation optimization for VLC NOMA-OMA system in multi-lamp multi-user scenarios. In *Proc. Int. Conf. Intelligent Computing and Wireless Optical Communications (ICICWOC)*, pages 71–75, 2024.

[8] N. Chi, H. Haas, M. Kavehrad, et al. Visible light communications: demand factors, benefits and opportunities [Guest Editorial]. *IEEE Wireless Communications*, 22(2):5–7, 2015.

[9] H. Marshoud, V. M. Kapinas, G. K. Karagiannidis, and S. Muhaidat. Non-Orthogonal Multiple Access for Visible Light Communications. *IEEE Photonics Technol. Lett.*, 28:51–54, 2015.

[10] J. Shi, J. He, K. Wu, and J. Ma. Enhanced Performance of Asynchronous Multi-Cell VLC System Using OQAM/OFDM-NOMA. *J. Lightware Technol.*, 37:5212–5220, 2019.

[11] X. Zhang and M. Haenggi. The Performance of Successive Interference Cancellation in Random Wireless Networks. *IEEE Trans. Inf..*, 60(20):6368–6388, 2014.

[12] K. Fan, T. Komine, Y. Tanaka, et al. The effect of reflection on indoor visible light communication system utilizing white leds. In *The 5th International Symposium on Wireless Personal Multimedia Communications (WPMC)*, pages 611–615, September 2002.

[13] T. Douseki et al. A batteryless wireless system uses ambient heat with a reversible-power-source compatible cmos/soi dc-dc converter. In *ISSCC Digest of Technical Papers*, pages 388–389, February 2003.

[14] O. Ergul, E. Dinc, and O. B. Akan. Communicate to illuminate: State-of-the-art and research challenges for visible light communications. *Physical Communication*, 17:72–85, 2015.

[15] Cheng-Chung Lee. *The current trends of optics and photonics*, volume 129. Springer, 2014.

[16] R. F. Fernandes, C. Fonseca, D. Brandão, et al. Flexible wireless sensor network for smart lighting applications. In *Instrumentation & Measurement Technology Conference (I2MTC)*. IEEE, 2014.

[17] Hoa Le Minh, D. O'Brien, G. Faulkner, et al. 100-mb/s nrz visible light communications using a postequalized white led. *IEEE Photonics Technology Letters*, 21(15):1063–1065, 2009.

[18] A. H. Azhar, T. A. Tran, and D. O'Brien. Demonstration of high-speed data transmission using mimo-ofdm visible light communications. In *IEEE Globecom 2010 Workshop on Optical Wireless Communications*, page 1052, 2010.

[19] J. Vucic, C. Kottke, S. Nerreter, et al. 513 mbit/s visible light communications link based on dmt-modulation of a white led. *Journal of Lightwave Technology*, 28(24):3512–3518, 2010.

[20] J. Vucic, C. Kottke, K. Habel, et al. 803 mbit/s visible light wdm link based on dmt modulation of a single rgb led luminary. *Journal of Lightwave Technology*, 2011.

[21] Harald Haas. LiFi is a paradigm-shifting 5g technology. *Reviews in Physics*, 3:26–31, 2018.

[22] A. M. Khalid, R. Cossu, R. Corsini, et al. 1-gb/s transmission over a phosphorescent white led by using rate-adaptive discrete multitone modulation. *IEEE Photonics Journal*, 4(5):1465–1473, 2012.

[23] D. Tsonev, H. Chun, S. Rajbhandari, et al. A 3-gb/s single-led ofdm-based wireless VLC link using a gallium nitride. *IEEE Photonics Technology Letters*, 26(7):637–640, 2014.

[24] H. Chun, S. Rajbhandari, G. Faulkner, et al. LED based wavelength division multiplexed 10 gb/s visible light communications. *Journal of Lightwave Technology*, 34(13):3047–3052, 2016.

[25] J. Beysens, A. Galisteo, Q. Wang, et al. DenseVLC: A cell-free massive MIMO system with distributed LEDs. In *The 14th International Conference*, 2018.

[26] J. Wang, A. Al-Kinani, W. Zhang, et al. A general channel model for visible light communications in underground mines. *China Communications*, 15(9):95–105, 2018.

[27] X. Wu and H. Haas. Load balancing for hybrid lifi and wifi networks: To tackle user mobility and light-path blockage. *IEEE Transactions on Communications*, 68(3):1675–1683, 2020.

[28] H.Haas, L.Yin, Y.Wang, and C.Chen. What is lifi? *Journal of lightwave technology*, 34(6):1534–1544, 2015.

[29] Koji Ohnai. Basic Technology of Optical Wireless OFDM System. *WBS Research Group Proposal*, 13(1):38–46, 2019.

[30] C. He and J. Armstrong. Clipping noise mitigation in optical OFDM systems. *IEEE Commun. Lett.*, 21(3):548–551, 2016.

[31] C. He, T. Q. Wang, and J. Armstrong. Performance of optical receivers using photodetectors with different fields of view in a MIMO ACO-OFDM system. *J. Lightwave Technol.*, 33(23):4957–4967, 2015.

[32] S. D. Dissanayake and J. Armstrong. Comparison of ACO-OFDM, DCO-OFDM and ADO-OFDM in IM/DD systems. *J. Lightwave Technol.*, 31(7):1063–1072, 2013.

[33] J. Armstrong and A. J. Lowery. Power efficient optical OFDM. *Electron. Lett.*, 42(6):370–372, 2006.

[34] Yang TU, Cuiwei HE, Yuto LIM, and TAN Yasuo. Performance of Asymmetrically Clipped DC Biased Optical OFDM in a NOMA-Based Visible Light Communication System. *IEICE Tech. Rep.*, 124(107):7–11, 2024. RCS2024-85, July 2024.

[35] Z. Dong, T. Shang, Q. Li, et al. Adaptive power allocation scheme for mobile noma visible light communication system. *Electronics*, 8(4):381, 2019.

[36] Shuang Chen, Kewu Peng, Huangpin Jin, et al. Analysis of outage capacity of noma: Sic vs. jd. *Journal of Tsinghua University (Natural Science Edition, English Version)*, 21(5):538–543, 2016.

[37] R. W. Chang. Orthogonal frequency multiplex data transmission system. U.S. Patent 3,488,445, 1966.

[38] L. J. Cimini. Analysis and simulation of a digital mobile channel using orthogonal frequency division multiplexing. *IEEE Trans. Commun.*, 33(7):665–675, 1985.

[39] S. Weinstein and P. Ebert. Data transmission by frequency-division multiplexing using the discrete Fourier transform. *IEEE Trans. Commun. Technol.*, 19(5):628–634, 1971.

[40] Suranga Dissanayake and John Armstrong. Comparison of aco-ofdm, dco-ofdm and ado-ofdm in im/dd systems. *Journal of Lightwave Technology*, 31(7):1063–1072, 2013.

[41] Ziaul Hasan, Hina Boostanimehr, and Vijay K. Bhargava. Green cellular networks: A survey, some research issues and challenges. *IEEE Communications Surveys & Tutorials*, 13(4):524–540, 2011.

[42] Guowang Miao, Nageen Himayat, Guoqiang Y. Li, and Shilpa Talwar. Energy-efficient link adaptation in frequency-selective channels. *IEEE Transactions on Communications*, 58(2):545–554, 2010.

List of Publications

[1] C. He, Y. Tu, and Y. Lim. "The Combination of SEFDM and NOMA in a Multi-User Visible Light Communication System". In *Opto-Elect. and Commun. Conf. (OECC)*, Melbourne, Australia, June 30–July 4 2024.

[2] Y. Tu, C. He, Y. Lim, and Y. Tan. "Performance Analysis for NOMA-based Multi-User VLC System". In *Joint Conf. of Hokuriku Chapters of Elect. and Inf. Soc. (JHES)*, pages E1–4–79, September 2024.

[3] Y. Tu, C. He, Y. Lim, and Y. Tan. "Performance of Asymmetrically Clipped DC Biased Optical OFDM in a NOMA-Based Visible Light Communication System". In *IEICE Tech. Committee on Radio Commun. Syst. (RCS)*, volume 124, pages 7–11, July 2024. RCS2024-85.

[4] Y. Tu, C. He, Y. Lim, and Y. Tan. "Optical OFDM-Based NOMA for Visible Light Communication(VLC)". In *IEICE Tech. Committee on Info. Netw. (IN)*, volume 124, pages 209–212, March 2025. IN2024-113.